Wang *et al. Metab Target Organ Damage*. 2025;5:23
DOI: 10.20517/mtod.2024.129

Metabolism and Target Organ Damage

Original Article

Open Access

Check for updates

Shared genetic architecture between metabolic dysfunction-associated steatotic liver disease and cardiometabolic traits comorbidities: a genome-wide pleiotropic and multi-omics study

Xuan-Yu Wang[1,2,#], Qiong Lyu[3,#], Yang-Yang Zhang[4,#], Yue Su[1], Hongjie Zhao[1], Hui-Hui Shen[5], Ying-Yu Xie[1,2]

[1]College of Traditional Chinese Medicine, Tianjin University of Traditional Chinese Medicine, Tianjin 301617, China.
[2]Tianjin Key Laboratory of Modern Chinese Medicine Theory of Innovation and Application, Tianjin University of Traditional Chinese Medicine, Tianjin 301617, China.
[3]Department of Oncology, Zhujiang Hospital, Southern Medical University, Guangzhou 510280, Guangdong, China.
[4]Shanghai Medical College, Fudan University, Shanghai 200032, China.
[5]Laboratory for Reproductive Immunology, Hospital of Obstetrics and Gynecology, Fudan University, Shanghai 200080, China
[#]Authors contributed equally.

Correspondence to: Dr. Ying-Yu Xie, College of Traditional Chinese Medicine, Tianjin University of Traditional Chinese Medicine, No. 10, Poyang Lake Road, Tuanpo Xinchengxi District, Jinghai District, Tianjin 301617, China. E-mail: xieyingyunn@163.com

How to cite this article: Wang XY, Lyu Q, Zhang YY, Su Y, Zhao H, Shen HH, Xie YY. Shared genetic architecture between metabolic dysfunction-associated steatotic liver disease and cardiometabolic traits comorbidities: a genome-wide pleiotropic and multi-omics study. *Metab Target Organ Damage*. 2025;5:23. https://dx.doi.org/10.20517/mtod.2024.129

Received: 10 Dec 2024 **First Decision:** 10 Mar 2025 **Revised:** 29 Mar 2025 **Accepted:** 8 Apr 2025 **Published:** 21 Apr 2025

Academic Editor: Amedeo Lonardo **Copy Editor:** Ting-Ting Hu **Production Editor:** Ting-Ting Hu

Abstract

Aim: While cardiometabolic disorders and metabolic dysfunction-associated steatotic liver disease (MASLD) frequently coexist, the genetic connections and causes are not clearly understood. This study aimed to explore their shared genetic architecture to elucidate the mechanisms driving their comorbidity.

Methods: Using summary statistics from genome-wide association studies (GWASs) on MASLD and 29 cardiometabolic traits (CMTs), we assessed their genetic correlation and causality, and identified shared genetic loci, genes, pathways, cell types, and tissues. Additionally, shared biological mechanisms were uncovered using single-cell RNA sequencing data.

Results: Significant genetic correlations were detected between MASLD and 17 CMTs, encompassing cardiometabolic diseases, glucose, lipids, adiposity, and inflammatory markers, after adjusting for multiple testing (*p*.adjust < 0.05). Cross-trait analysis yielded a total of 166 shared risk SNPs (including those located in or near *TRIB1*, *LPL*, *PNPLA3*, *GCKR*, and *PPARG*). Subsequent colocalization highlighted 73 genetic loci associated with both MASLD and CMTs, with rs429358 (*APOE*) consistently prioritized in HyPrColoc. Common genes were identified (such as *NPC1*, *MST1R*, *TMBIM1*, *IRAK1BP1*, *L3MBTL3*, *RBM6*, and *RGS19*), with significant enrichment in cholesterol metabolism, glucose metabolism, immune inflammation, and long-term depression. Shared tissue-specific heritability enrichment was identified in the liver, adipose, artery, adrenal gland, and brain tissue. Moreover, shared enrichment was observed in specific cell types (epicardial adipocytes, erythroid progenitor cells, hepatocytes, glial cells, macrophages, monocytes, and myeloid cells). The expressions of *APOE* and *LPL*, which showed colocalization between MASLD and CMTs, were significantly altered in the macrophages of patients with MASLD compared to those of controls. Causality and potential medications were also explored.

Conclusion: Multiple biological pathways contribute to the comorbidity between MASLD and cardiometabolic disorders, with lipid metabolism emerging as a critical factor. This study provides valuable insight into the possible mechanisms underlying their comorbidity and offers potential directions for future therapeutic innovations.

Keywords: Metabolic dysfunction-associated steatotic liver disease, cardiometabolic disease, cholesterol metabolism, macrophage, nonalcoholic fatty liver disease, obesity, shared genetic architecture, single-cell RNA sequencing

HIGHLIGHTS

· A large-scale study combines advanced genetic epidemiology methods with single-cell transcriptomics.
· Significant genetic correlations exist between MASLD and 17 CMTs.
· A total of 166 genomic risk loci and 73 shared causal variants for MASLD with these CMTs.
· Cholesterol metabolism, glucose metabolism, immune inflammation, and long-term depression are intricately co-enriched within the liver-heart axis.
· Genetic evidence supports drug repurposing candidates for MASLD and its comorbidities.

INTRODUCTION

Metabolic dysfunction-associated steatotic liver disease (MASLD) is the leading cause of cirrhosis and hepatocellular carcinoma worldwide[1], characterized by hepatic steatosis accompanied by at least one cardiometabolic risk factor. MASLD affects over 25% of the global population[2], with cardiometabolic disease being the most common cause of death among these patients[3]. MASLD has been introduced to replace previous terms, including nonalcoholic fatty liver disease (NAFLD) and metabolic dysfunction-associated fatty liver disease (MAFLD), to better reflect evolving diagnostic criteria for fatty liver disease with metabolic underpinnings[4].

In recent years, the liver-heart axis theory has garnered increasing attention[5,6], with a growing body of evidence indicating that cardiometabolic traits (CMTs) serve as independent risk factors for MASLD, while the reverse relationship is also observed[7-10]. For example, individuals diagnosed with MASLD exhibited a higher incidence of cardiovascular-related deaths compared to controls, as evidenced by the US National Health and Nutrition Examination Survey[11]. Conversely, among adults with one or more of these cardiometabolic diseases, the prevalence of MASLD rises steeply to over 60%-75%[12,13]. A prospective cohort study further reveals that individuals with liver cirrhosis experience a substantial burden of heart disease, detected on magnetic resonance imaging (MRI), characterized by myocardial inflammation, fibrosis, and impaired systolic function[14]. Moreover, a recent study reported that a genetically modified mouse model of

lean NAFLD reveals sexual dimorphism in the liver-heart axis[15]. Despite these advancing insights, however, and with emerging evidence increasingly suggesting the role of genetic factors in mediating these associations, the precise mechanisms driving this bidirectional detrimental interplay remain inadequately understood[16].

The recent decade's advancements in genetics, particularly through genome-wide association studies (GWASs), which analyze several hundred thousand to over a million single nucleotide polymorphisms (SNPs) in thousands of individuals, have provided new opportunities to evaluate a potential shared genetic foundation for MASLD and CMTs, prompting us to conduct this study[17-20]. While recognized MASLD variants have enhanced our understanding of the disease's etiology[21], they explain only 10%-20% of its heritable factors[22], underscoring the urgency for more comprehensive genetic investigations. Advances in GWAS have also yielded in-depth variant profiles for multiple CMTs, significantly deepening our understanding of these conditions[23]. The substantial heritability and polygenic nature of both MASLD and CMTs suggest a shared genetic foundation, which could pave the way for more precise diagnoses and safer, targeted treatments for each condition, both independently and when they co-occur.

CMTs were characterized as a multifaceted array of traits intricately associated with cardiometabolic health. We examined a total of 17 metabolic traits (comprising four glucose traits, three blood pressure traits, five lipid traits, three adiposity traits, and two inflammatory markers), along with three metabolic disorders and nine cardiometabolic disorders, all of which are closely linked to both MASLD and cardiometabolic disorders. Herein, we leveraged well-powered GWAS data to examine genetic correlations and potential causality between MASLD and CMTs. Following this, we performed genome-wide cross-trait analysis to identify potential risk loci and elucidate the underlying common genetic foundations. A comprehensive post-GWAS analysis was conducted to reveal common genetic variants, enriched pathways, relevant cell types, and tissues. Notably, we investigated genomic regions showing evidence of locus-level correlations by estimating colocalization among various traits using the novel hypothesis prioritization for multi-trait colocalization (HyPrColoc) methodology to ascertain whether co-causal variants exist in these regions[4]. Additionally, we explored the variability of shared pathways across different cell types in MASLD patients at the single-cell level. Lastly, we utilized drug-gene databases to pinpoint several cardiometabolic medications with high potential for treating MASLD alongside comorbidities. A systematic flow of the study design can be found in Figure 1.

METHODS

GWASs summary data

We collected GWAS summary data about MASLD, along with 12 cardiometabolic diseases, 15 metabolic traits, and two inflammatory markers. These traits manifest across various conditions, including liver fat accumulation, excess weight, diabetes, metabolic irregularities, and immune responses. The largest GWAS dataset for MASLD to date was derived from a meta-analysis of four cohorts with electronic health record-documented MASLD, comprising 8,434 cases with hepatic steatosis, MASH (metabolic dysfunction associated steatohepatitis), or liver fibrosis, and 770,180 controls[24]. Most cardiometabolic diseases were analyzed in over 10,000 case samples, while metabolic traits and inflammatory markers were assessed in at least 100,000 individuals. While European ancestry predominated, a few studies incorporated diverse ancestral groups. These datasets exhibit cutting-edge potential for identifying genetic susceptibility to MASLD and CMTs by analyzing common SNPs. Utilizing these datasets, we created analysis frameworks to shed light on the genetic similarities between MASLD and CMTs, focusing on shared SNPs, genes, pathways, tissues, and various cell types. Supplementary Table 1 provides a comprehensive overview of the features associated with each dataset included in the study.

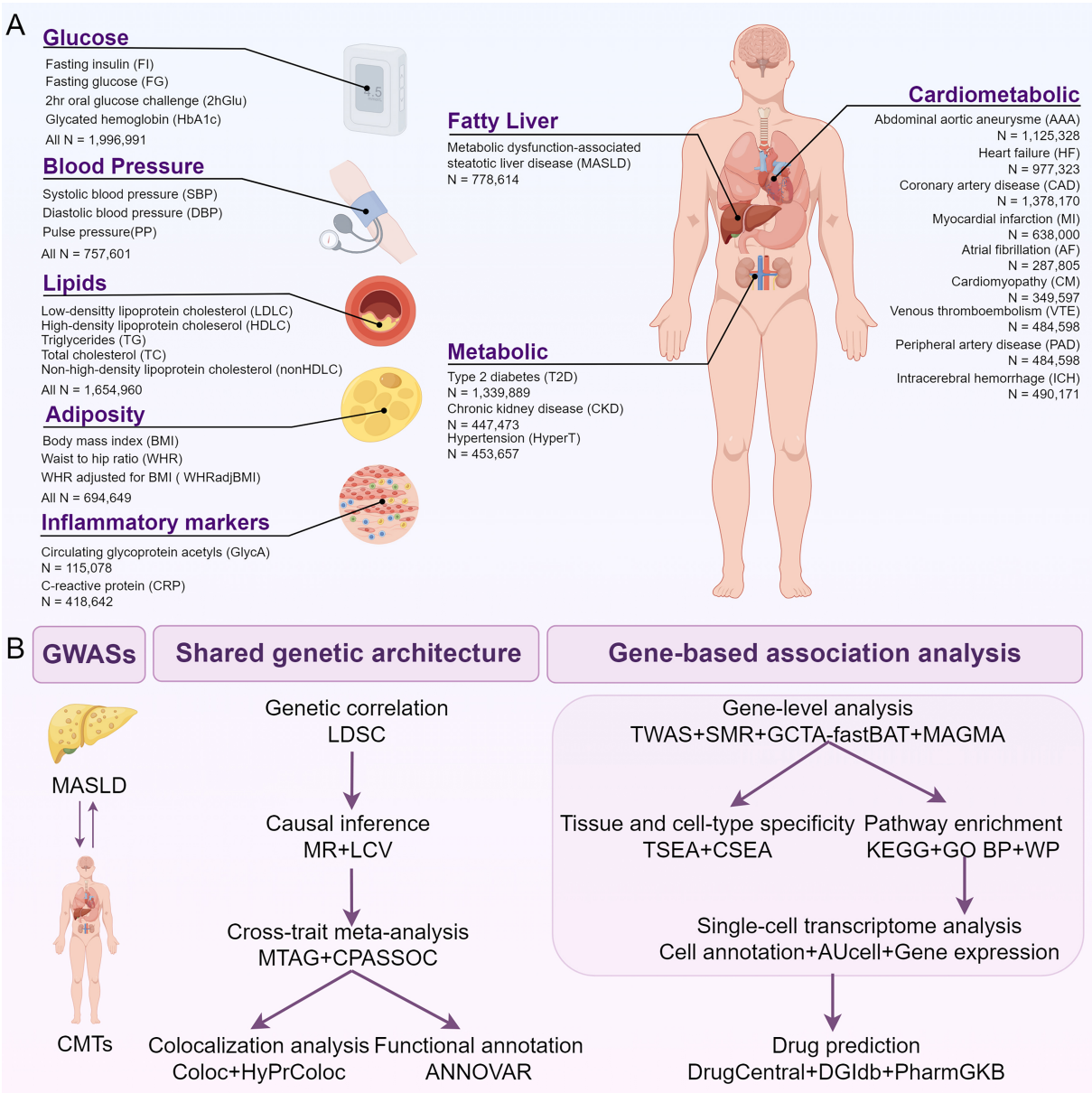

Figure 1. Schematic overview of study design. (A) Overview of traits and data sources. This panel details the trait categories, abbreviations, and sample sizes for MASLD and 17 metabolic traits (comprising four glucose traits, three blood pressure traits, five lipid traits, three adiposity traits, and two inflammatory markers), three metabolic disorders, and nine cardiometabolic disorders, based on GWAS results utilized in the genetic pleiotropy analysis; (B) Study workflow. This panel outlines the analytical framework, including the following modules: computation of genome-wide genetic correlations, inference of causality using bidirectional MR, identification of shared causal variants, genes, and pathways, detection of tissues and cell types most affected by shared genetic signals, single-cell transcriptome analysis, and prioritization of therapeutic drugs targeting MASLD complications. MASLD: Metabolic dysfunction-associated steatotic liver disease; GWASs: genome-wide association studies; CMTs: cardiometabolic traits; LDSC: linkage disequilibrium score regression; MR: Mendelian Randomization; LCV: Latent Causal Variable; MTAG: multi-trait analysis of GWAS; CPASSOC: cross-phenotype association test; TWAS: transcriptome-wide association study; SMR: summary-data-based Mendelian Randomization; GCTA-fastBAT: a fast set-based association analysis; MAGMA: Multi-marker Analysis of GenoMic Annotation; TSEA: tissue-specific expression analysis; CSEA: cell type-specific enrichment analysis; KEGG: Kyoto Encyclopedia of Genes and Genomes; GO: gene ontology; BP: biological process; WP: WikiPathways. This figure was made with Figdraw (https://www.figdraw.com/).

Genetic correlation analysis

We evaluate the global genetic correlations between MASLD and CMTs using linkage disequilibrium score

regression (LDSC)[25]. Adhering to the LDSC methodology, we accessed pre-calculated LD scores derived from the European reference panel of the 1,000 Genomes Project Phase 3, limiting our analysis to haplotype map 3 (HapMap3) SNPs to lessen the bias introduced by low imputation quality. The genetic correlation (r_g) varies from -1 to 1, where -1 signifies a perfect negative correlation and 1 denotes a perfect positive correlation. The Benjamini-Hochberg method was employed to calculate the false discovery rate (FDR) for multiple testing (FDR < 0.05).

Mendelian randomization analysis

Next, we assessed the bidirectional causal relationship between MASLD and CMTs using the Mendelian Randomization (MR) analysis method. Inverse-variance weighting (IVW) was adopted as our principal methodology[26]. To enhance the IVW analysis, we implemented MR-Egger[27], simple mode, weighted median[28], weighted mode, and MR-APSS[29] strategies to scrutinize the strength and coherence of the results. For IVW, MR-Egger, simple mode, weighted median, and weighted mode, we applied a genome-wide significance threshold of $P = 5 \times 10^{-8}$ and an F-statistic above 10, while using the default $P = 5 \times 10^{-5}$ threshold for MR-APSS in instrument selection. Independent SNPs were selected using LD clumping ($r^2 < 0.001$ within 1,000 kb) with PLINK v3[30], focusing on the 1,000 Genomes Project Phase 3 (European). Furthermore, we referred to the GWAS Catalog (https://www.ebi.ac.uk/gwas/) to filter out SNPs connected to the outcome and its risk factors such as smoking behavior and alcohol consumption. Cochran's *Q*-test assessed heterogeneity, and the MR-Egger intercept was used to evaluate horizontal pleiotropy. The MR analyses were conducted using the TwoSampleMR[31] and MRAPSS[29] R packages. To alleviate the impact of multiple testing, we employed a Benjamini-Hochberg correction (FDR < 0.05). To mitigate potential bias due to overlapping samples, GWAS data for both exposure and outcome were obtained from distinct cohorts.

Genetic causality proportion

Genetic correlations might impact bidirectional causality, causing false associations. To tackle this concern, the Latent Causal Variable (LCV) method was utilized to estimate the genetic causality proportion (GCP) and verify the MR results[32]. GCP quantifies the ratio of the possible causal influence to the genetic correlation, where both positive and negative values signify the direction of the causal effect. The statistical significance of GCP was indicated by $P < 0.05$.

Cross-trait meta-analysis

To detect pleiotropic loci in MASLD and CMTs, we conducted two cross-trait meta-analyses, including a multi-trait analysis of GWAS (MTAG)[33] and a cross-phenotype association test (CPASSOC)[34]. Drawing on a strong genetic correlation between two traits, MTAG carries out a meta-analysis of diverse traits, contingent upon the premise that all variants display identical genetic correlation across all traits involved. Despite the possibility of overlapping samples in GWAS summary statistics for different characteristics, MTAG yields effective results. To explore the assumptions on equal variance-covariance, we calculated the maximum false discovery rate (maxFDR).

CPASSOC conducts a sensitivity analysis by integrating association evidence from the GWAS summary statistics of multiple traits, provided that the variant is correlated with at least one trait. CPASSOC offers two statistical tests, SHom and SHet. Although SHom is strongest with uniform genetic effect sizes, this assumption is often breached in meta-analyses of multiple traits. SHet, an extension of SHom, preserves statistical power even with heterogeneity. Hence, we applied the SHet estimate to infer heterogeneous effects across different traits. To derive independent SNPs, we utilized the PLINK clumping function with parameters: --clump-p1 5e-8, --clump-p2 1e-5, --clump-r2 0.2, and --clump-kb 500. Significant shared SNPs were defined as loci that achieved genome-wide significance in both MTAG and CPASSOC ($P < 5 \times$

10^{-8}) and suggestive significance for each trait GWAS ($P < 1 \times 10^{-3}$). ANNOVAR[35] annotated variants identified by MTAG and CPASSOC.

Colocalization analysis

We performed a colocalization analysis using Coloc[36] to determine if the same variants account for two GWAS signals or if they are distinct variants in proximity to one another. For each of the 166 shared SNPs between MASLD and CMTs, variants within 500 kb of the index SNP were extracted, and the probability of a shared causative variant for the two traits was computed (PP.H4, the posterior probability for H4). If PP.H4 was more than 0.7, the locus was regarded as colocalized. With the Bayesian method HyPrColoc[4], which efficiently manages the colocalization of multiple traits, we determined the posterior probability of various traits sharing the same SNP. Colocalization results were visualized using the GENI plots R package (https://github.com/jrs95/geni.plots).

Gene-based association analysis

In most cases, SNP mutations do not yield effective genetic information. Hence, besides annotating genes using ANNOVAR, we also used transcriptome-wide association study (TWAS)-fusion[37], Summary-data-based Mendelian Randomization (SMR)[38], GCTA-fastBAT[39], and Multimarker Analysis of GenoMic Annotation (MAGMA)[40] to discover genes shared by MASLD-CMTs trait pairs. All four gene-level analyses utilized the entire GWAS summary statistics from MTAG in the meta-analysis as input files. The gene-based analysis incorporated the European ancestry panel derived from the 1,000 Genomes Project (Phase 3). In addition, we employed the Benjamini-Hochberg method for adjusting *P*-values across multiple tests in each technique. FDR < 0.01 was used to determine statistical significance.

To explore the associations between MASLD and CMTs regarding gene expression in specific tissues, we conducted a TWAS using FUSION[37], integrating GWAS summary data with expression weights across 49 tissues[41]. Furthermore, to strengthen the efficacy of the TWAS, we conducted a sparse canonical correlation analysis (sCCA)-TWAS[42] utilizing cross-tissue reference panels. Single-tissue TWAS and sCCA-TWAS were combined using an aggregate Cauchy association test (ACAT).

SMR[38] utilizes GWAS summary data alongside expression quantitative trait loci (eQTL) study data to identify genes whose expression levels are associated with intricate traits through pleiotropy. SMR employs the HEIDI tests to separate causality from the linkage. Using cis-eQTL summary data, we executed SMR with Genotype-Tissue Expression project (GTEx) V8 for whole blood and nine relevant tissues, including adipose subcutaneous, artery aorta, artery coronary, artery tibial, heart atrial appendage, heart left ventricle, kidney cortex, liver, and lung. Genes with an FDR < 0.01 and a $P_{HEIDI} > 0.01$ were marked as significant.

GCTA-fastBAT[39], a fast set-based association analysis, examines human complex traits by utilizing summary data from GWAS and LD data from a reference sample with individual genotypes. The gene-trait associations were analyzed only for SNPs located within the gene.

MAGMA[40] applies a multiple regression framework to appropriately account for LD between markers and recognize multi-marker effects. Power can be significantly increased through gene-based association by collecting signals across variants in target regions when multiple causal variants affect the phenotype. MAGMA was run using default parameters, annotating variants to 20,259 protein-coding genes from the Ensembl v110 release.

Pathway enrichment analysis

To investigate the biological pathways of these shared genes within the liver-heart axis, we performed a pathway enrichment analysis that drew from the Gene Ontology (GO), Kyoto Encyclopedia of Genes and Genomes (KEGG), and WikiPathways (WP) databases, applying the clusterProfiler[43] R package. With a Benjamini-Hochberg correction, pathways were identified as significant (FDR < 0.05).

Tissue-specific expression analysis

Tissue-specific expression analysis (TSEA)[44] was conducted to determine if genes shared by MASLD-CMTs trait pairs are highly expressed in tissues related to the disease. The GTEx provided publicly available expression data for the tissue enrichment of genes found in the four gene-based analyses. The GTEx project involves 1,839 samples from 189 deceased individuals, covering 45 different tissues, and some tissues have multiple "sub-tissue" types. The Benjamini-Hochberg correction was employed to compensate for multiple comparisons (FDR < 0.05).

Cell-type-specific enrichment analysis

To analyze the cell-type enrichment of genes shared by MASLD-CMTs trait pairs, we employed the Web-based Cell-type Specific Enrichment Analysis of Genes (WebCSEA)[45]. Employing the decoding tissue-specificity (deTS) algorithm, WebCSEA compiled 111 single-cell RNA-seq (scRNA-seq) panels of human tissues and 1,355 tissue-cell types (TCs) from 61 overall tissues across 11 human organ structures. Fisher's exact test was used to assess if the genes common with each phenotype pair were overrepresented among the cell type-specific genes.

Single-cell RNA sequencing analysis

MASH denotes an advanced stage of MASLD marked by hepatocyte damage, inflammation, and hepatic fibrosis. Access to the scRNA-seq data for MASH was gained through the GSE129516[46] dataset in the Gene Expression Omnibus (GEO) database, comprising samples from the Chow and MASH groups. After filtering out doublets and poor-quality cells, 33,168 cells with expression of more than 500 genes were utilized for further analysis. We employed the Seurat[47] R package (version 4.3.0) to perform normalization, integration, dimensional reduction, and clustering, enabling us to distinguish various subsets. Batch effects were mitigated using the top 20 PCA components with the harmony[48] R package (version 1.2.1). All clustered cells were visualized and analyzed using the t-distributed Stochastic Neighbor Embedding (t-SNE) algorithm. Cell type annotation was performed utilizing the SingleR[49] R package, which enables the comparison of gene expressions across several cell types with single-cell gene expressions. To calculate the activity score of the shared pathways at the cellular level, the AUcell[50] algorithm was applied, with the results visualized through t-SNE plots and boxplots.

Cardiometabolic medications for MASLD

By designating the genes recognized by all four gene-based analyses as disease genes for each MASLD-CMTs trait pair, we discovered a total of 356 disease genes. ClusterProfiler[43] was applied to explore shared genes and ascertain the pathological pathways enriched for each MASLD trait pair, aiming to identify drugs that best correspond with the genes. Next, we conducted two stages to identify potential medications for examination: (1) We searched three extensive drug-gene databases, DGIdb[51], DrugCentral[52], and PharmGKB[53], for pharmaceuticals that target any of the 356 candidate genes; (2) The compounds approved by the US Food and Drug Administration (FDA) were restricted to those already utilized in standard clinical practices for treating cardiometabolic diseases, resulting in approximately 48 drugs.

Statistical analysis

The primary environment for our statistical analysis was Linux, where we used R, Python, and Plink. The ggraph R package was employed to visualize the shared SNPs in a circular dendrogram. In addition, the Benjamini-Hochberg method was employed to get the FDR for adjusting *P*-values in multiple tests. The Wilcoxon test was applied to estimate statistical significance in comparisons between two groups.

RESULTS

Genetic correlation

Positive correlations between MASLD and 17 CMTs were found by LDSC after adjusting for multiple testing [Figure 2A]. Adiposity emerged as the trait most strongly correlated, with the waist-to-hip ratio (WHR, $r_g = 0.88$, $P = 3.8 \times 10^{-6}$) being the highest, followed by body mass index (BMI) and WHR adjusted for BMI (WHRadjBMI, $r_g > 0.5$, $P < 2.5 \times 10^{-5}$). Regarding cardiometabolic disease, type 2 diabetes (T2D, $r_g = 0.87$, $P = 1.2 \times 10^{-5}$) was the most pertinent, with others including myocardial infarction (MI), hypertension (HyperT), coronary artery disease (CAD), heart failure (HF), peripheral artery disease (PAD), venous thromboembolism (VTE), atrial fibrillation (AF), and abdominal aortic aneurysm (AAA, $r_g > 0.25$, $P < 0.03$). Additionally, among the lipid and glucose metrics, triglycerides (TG), fasting insulin (FI), and non-HDL cholesterol (nonHDLC) were significantly connected to MASLD in a descending sequence ($r_g > 0.3$, $P < 0.02$). Only diastolic blood pressure (DBP) among the blood pressures exhibited a minor genetic correlation with MASLD, which did not survive after adjusting multiple tests ($r_g = 0.17$, $P = 0.039$, Figure 2A).

Causal association

Bidirectional MR was conducted to investigate the possible causal effects and to evaluate if the genetic commonality between MASLD and CMTs corresponds with pleiotropy [Figure 2B]. As expected, adiposity traits demonstrated the strongest causal relationships with MASLD, including BMI (OR = 1.64, $P = 3 \times 10^{-27}$), WHR (OR = 1.78, $P = 6 \times 10^{-20}$), and WHRadjBMI (OR = 1.47, $P = 2 \times 10^{-10}$). Notably, T2D demonstrated a bidirectional causal relationship with MASLD, with T2D increasing MASLD risk (OR = 1.19, $P = 5 \times 10^{-6}$) and MASLD elevating T2D risk (OR = 1.24, $P = 0.005$). MR-APSS further validated the causal link between BMI, WHR, WHRadjBMI, and T2D with MASLD. Additionally, HyperT (OR = 1.11, $P = 8 \times 10^{-4}$) and TG (OR = 1.45, $P = 4 \times 10^{-10}$) showed positive causal links with MASLD. Conversely, MASLD was found to causally influence DBP (OR = 1.61, $P = 0.002$) and FI (OR = 1.03, $P = 5 \times 10^{-7}$). No notable horizontal pleiotropy was found using MR Egger, and heterogeneity was absent.

Considering genetic correlation and potential sample overlap in MR analysis, LCV was used to assess GCP values for MASLD trait pairs with significant MR outcomes [Table 1]. Four trait pairs showed statistical significance and demonstrated a strong causal link ($|GCP| \geq 50\%$, $P \leq 3 \times 10^{-3}$). For the MASLD-DBP pair, LCV estimates were consistent with the directional findings from the MR analysis. In contrast, the LCV estimates for the other three obesity traits (BMI, WHR, and WHRadjBMI) associated with MASLD diverged from the directions observed in the MR analysis. This inconsistency suggests a complex bidirectional interplay between obesity and MASLD, potentially indicative of a deleterious feedback loop warranting further exploration.

Cross-trait loci and causal variants

Using MTAG and CPASSOC for cross-trait meta-analysis, we discovered 166 SNPs common to the 17 MASLD-CMTs trait pairs [Supplementary Table 2]. In total, MASLD shares the highest number of SNPs with nonHDLC (N = 28) and TG (N = 26) and then with adiposity traits, which have about 13 to 21 SNPs in common [Figure 3A]. Then, coloc was employed to colocalize these SNPs across traits and identify shared causal variants. This analysis revealed 73 causal variants associated with both traits within the liver-heart

Table 1. Partial causality evaluation employing the Latent Causal Variable framework

Trait1	Trait2	GCP	SE	*P*
MASLD	DBP	0.83	0.12	4×10^{-41}
MASLD	BMI	0.50	0.41	9×10^{-5}
MASLD	WHR	0.76	0.21	2×10^{-4}
MASLD	WHRadjBMI	0.68	0.22	3×10^{-3}

MASLD: Metabolic dysfunction-associated steatotic liver disease; GCP: genetic causal proportion; SE: standard error; *P*: *P*-value; DBP: diastolic blood pressure; BMI: body mass index; WHR: waist-to-hip ratio; WHRadjBMI: WHR adjusted for BMI.

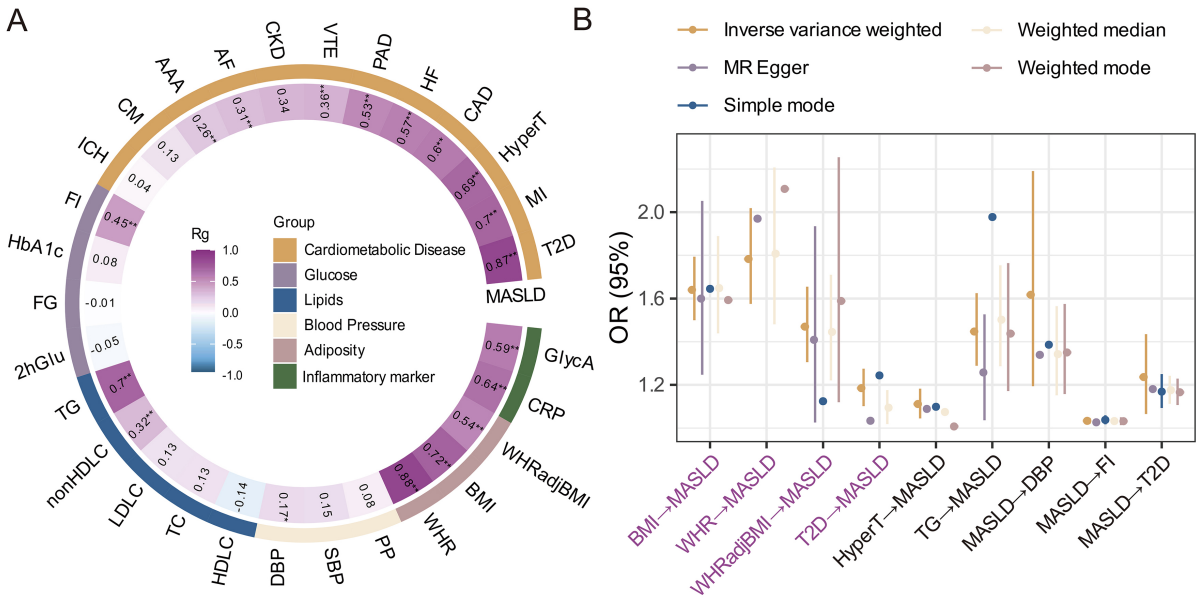

Figure 2. Genetic correlation and causal relationship between MASLD and CMTs. (A) The genetic correlation (r_g) derived from LDSC was displayed on this heatmap, using colors to show the correlation's strength, $^{*}P < 0.05$; **FDR < 0.05; (B) Causal relationships were inferred using two-sample MR employing five distinct methods. MR-APSS validated causalities and labeled them using the purple font. Dots illustrate the OR, and the color bars represent the 95% confidence intervals. MASLD: Metabolic dysfunction-associated steatotic liver disease; CMTs: cardiometabolic traits; LDSC: linkage disequilibrium score regression; FDR: false discovery rate; MR: Mendelian Randomization; OR: odds ratios; r_g: genetic correlation.

axis [Supplementary Table 3]. HyPrColoc identified five causal variants shared across multiple traits [Figure 3B and Supplementary Table 4]. *APOE* was prioritized as the causal gene at this locus based on a cluster of colocalizing phenotypes, including MASLD, T2D, WHR, and WHRadjBMI, with rs429358 emerging as the most probable (PP = 99.9% for a shared signal across traits) underlying causal variant [Figure 3C]. Notably, rs58542926 (*TM6SF2*) showed strong multi-trait colocalization between MASLD and six traits (T2D, nonHDLC, TG, WHRadjBMI, CRP, and GlycA), while rs112875651 (*TRIB1*) similarly demonstrated colocalization between MASLD and eight traits (CAD, MI, nonHDLC, TG, BMI, WHR, WHRadjBMI, and GlycA), all of which are linked to lipid metabolism, obesity, and inflammation within the liver-heart axis.

We found that shared SNPs within the liver-heart axis, whether causal or not, were concentrated near genes involved in lipid and glucose metabolism, particularly cholesterol metabolism [Supplementary Table 5]. For instance, *TRIB1* was the nearest gene to nine SNPs that were common between MASLD and ten additional traits, where rs112875651 and rs2980885 were shared across three trait pairs, and two trait pairs shared

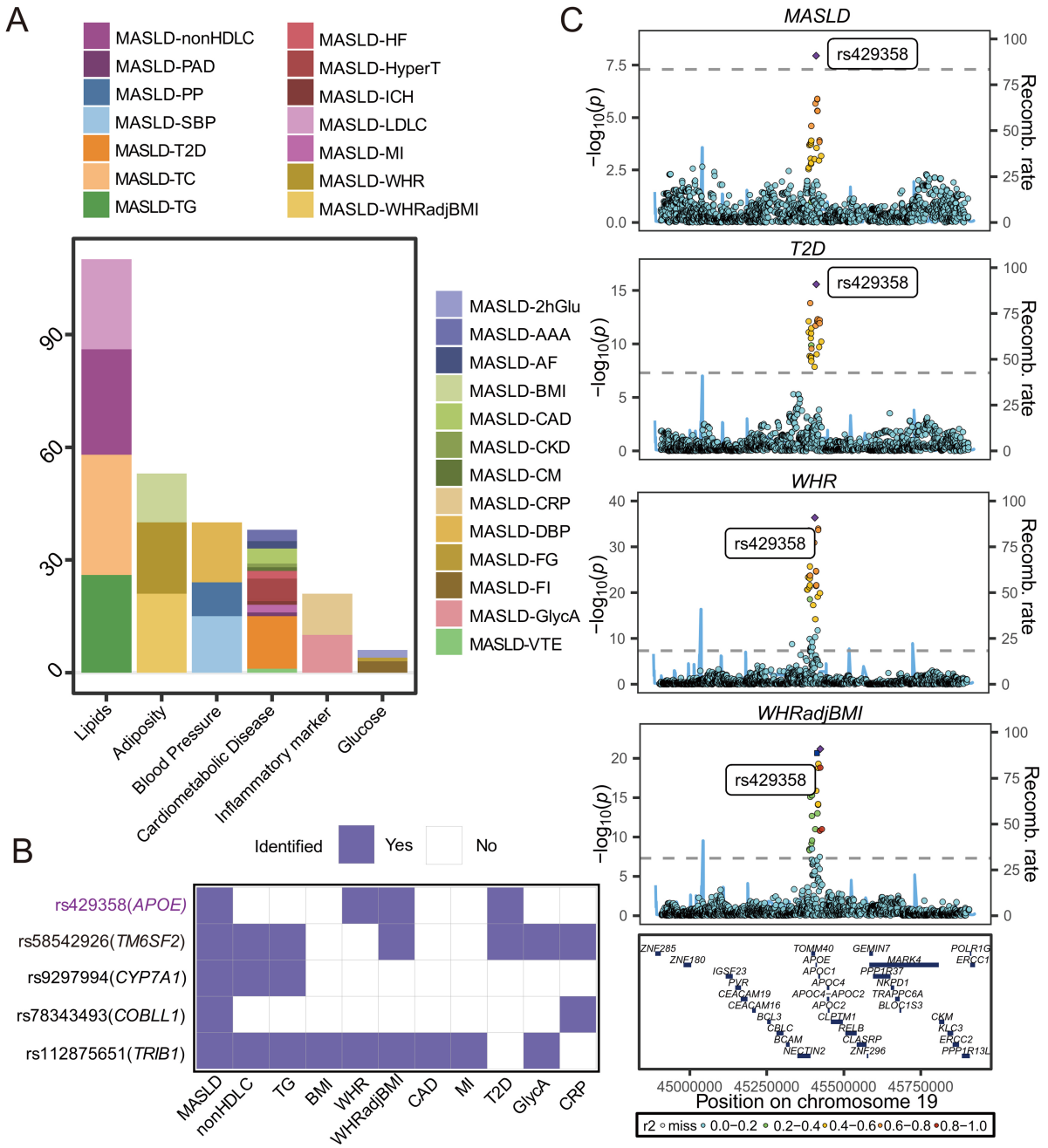

Figure 3. The general overview of the pleiotropic links between MASLD and CMTs. (A) Count of shared SNPs between MASLD and CMTs using MTAG and CPASSOC; (B) HyPrColoc identified five causal variants that are common across multiple traits; (C) LocusZoom visualizations of rs429358 causal variant for MASLD and three CMTs, including T2D, WHR, and WHRadjBMI. The X-axis displays the chromosomal locations of SNPs, and the Y-axis represents the negative base 10 logarithm of *P*-values [$-\log_{10}(p)$] from two-sided statistical analyses. MASLD: Metabolic dysfunction-associated steatotic liver disease; CMTs: cardiometabolic traits; T2D: type 2 diabetes; WHR: waist-to-hip ratio; WHRadjBMI: WHR adjusted for BMI; MTAG: multi-trait analysis of GWAS; CPASSOC: cross-phenotype association test; SNPs: single nucleotide polymorphisms; BMI: body mass index; VTE: venous thromboembolism; TG: triglyceride; nonHDLC: non-HDL cholesterol; MI: myocardial infarction; HyperT: hypertension; CAD: coronary artery disease; HF: heart failure; PAD: peripheral artery disease; AF: atrial fibrillation; FI: fasting insulin; AAA: abdominal aortic aneurysm; DBP: diastolic blood pressure.

rs2980854. *LPL* was related to six common SNPs across nine trait pairs, with rs15285 being a causal SNP for

two trait pairs. Likewise, *FTO* was linked to six SNPs common to eight trait pairs., including rs17817964, which was causal for three pairs of traits. Interestingly, *SUGP1*, identified as a novel regulator of cholesterol metabolism, and *PNPLA3*, recognized as a triglyceride lipase, were each associated with three SNPs and linked to seven and eight trait pairs, respectively. In addition, rs1260326 and rs62131879 on *GCKR* were discovered to be associated with glucose regulation and related to MASLD with HyperT, CRP, GlycA, and nonHDLC. *PPARG* was crucial in lipid metabolism and inflammatory responses, and it was associated with two SNPs prevalent in three trait combinations: MASLD with WHR, WHRadjBMI, and TG. Finally, multiple shared causal SNPs were located near the genes *APOE*, *TM6SF2*, *CYP7A1*, *COBLL1*, and *TRIB1*, all involved in lipid regulation and associated with MASLD and its complications.

Although the genetic correlation between DBP and MASLD was modest, MR and LCV analyses revealed that MASLD may contribute to changes in DBP, suggesting that impaired MASLD-induced DBP influences the liver-heart axis. To further investigate this relationship, we utilized MTAG and CPASSOC to identify and validate shared genetic loci between MASLD and DBP, thereby uncovering potential therapeutic targets, including *CACNB2*, *PELI1*, *TRIB1*, *PNPLA3*, *PLCE1*, and *COBLL1*.

Gene-based association analysis

Determining gene associations for GWAS variants solely based on proximity is a simplistic approach that overlooks the role of pleiotropy. We opted for four different methods, including TWAS-fusion, SMR, GCTA-fastBAT, and MAGMA, to identify shared genes within the liver-heart axis [Figure 4A]. eQTL are employed by the first two methods, whereas the last two focus on proximity for conducting gene burden tests. A total of 356 disease genes were defined using all four methods [Supplementary Table 6], and 38 of these were linked to at least three MASLD-CMTs trait pairs [Figure 4B]. Remarkably, the genes *NPC1*, *MST1R*, *TMBIM1*, *IRAK1BP1*, *L3MBTL3*, *RBM6*, and *RGS19* were found to be shared across five or more pairs of traits associated with MASLD-CMTs. Such a wide distribution indicates crucial roles in liver-heart axis interactions and metabolic regulation. Notably, *NPC1*, *MST1R*, and *TMBIM1* are significantly associated with lipid metabolism, whereas *IRAK1BP1* and *L3MBTL3* are connected to inflammatory responses. Moreover, *RBM6* and *RGS19* may play significant roles in advancing hepatocellular carcinoma.

Biological pathways and mechanisms

Through the exploration of biological pathways with genes sourced from four diverse methodological techniques, we identified substantial enrichment in lipid and glucose metabolism, endocrine disorders, and immune inflammation, grounded in etiological mechanisms within the liver-heart axis [Figure 4C]. Among lipid metabolism pathways, cholesterol metabolism stood out as the most significantly enriched, with subsequent pathways including bile secretion, lipid and atherosclerosis, sphingolipid signaling, and steroid hormone biosynthesis. This underscores the potentially critical role of lipid metabolism abnormalities in mediating the liver-heart axis, which may contribute to severe systemic comorbidities. Interestingly, insulin resistance, glucagon signaling pathway, and maturity-onset diabetes of the young were also significantly enriched, indicating that glucose metabolic abnormalities might play a role in MASLD comorbidities like T2D. Cellular senescence played a crucial role in various cellular processes and was significantly implicated in the pathological progression of MASLD and cardiometabolic disorders, particularly associated with endoplasmic reticulum (ER) stress. Malignant tumors, particularly pancreatic and hepatocellular carcinoma, were also notably enriched, underscoring the potential of the liver-heart axis to lead to serious complications that impose substantial socio-medical burdens, warranting further investigation and validation. Given the central role of metabolic abnormalities in the comorbidity of MASLD and CMTs, we conducted a WP enrichment analysis on the shared targets of each trait pair. In alignment with prior findings, nearly all trait pairs of shared genes exhibited significant lipid metabolism enrichment, explicitly cholesterol metabolism among conditions such as MASLD with HF, CAD, AAA, TG, nonHDLC, and CRP [Supplementary Figure 1].

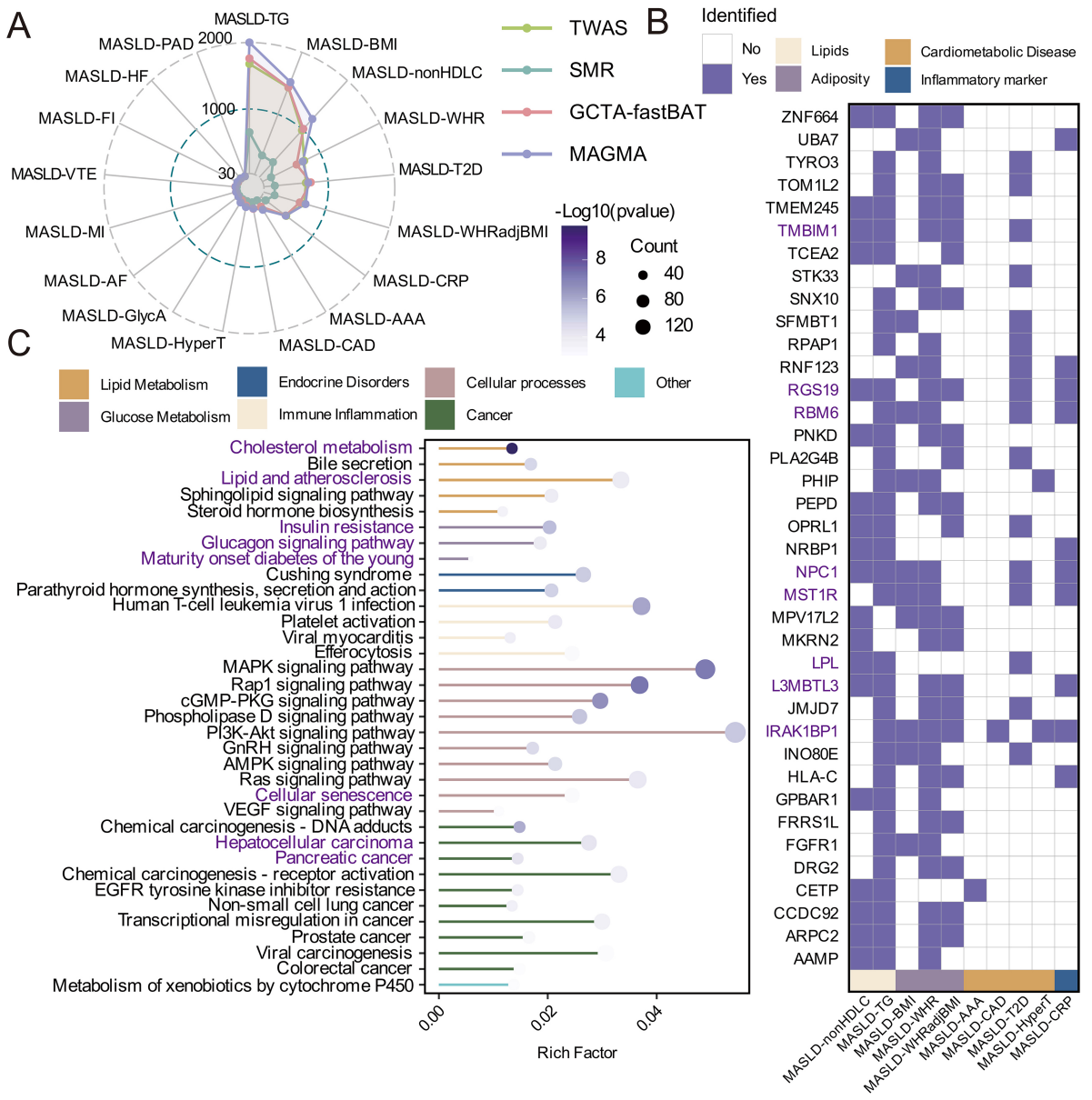

Figure 4. The shared genes and pathways for MASLD and CMTs. (A) Using TWAS, SMR, GCTA-fastBAT, and MAGMA, the number of genes for each MASLD-CMTs trait pair was identified. Distinct colors are allocated to each method, with the number of identified genes clearly labeled on each level. To correct for multiple testing, the FDR adjustment was applied; (B) Genes are presented with all four gene-centric analysis methods identified and shared by at least three MASLD-CMTs trait pairs. The bottom of the figure shows the trait pairs, while the left side displays the genes. The purple color signifies the presence of genes. FDR correction was utilized to correct for multiple tests in each analysis; (C) Biological mechanisms categorize the KEGG pathway enrichment of genes shared by MASLD and CMTs. Pathways with FDR < 0.05 in the hypergeometric test were all included. MASLD: Metabolic dysfunction-associated steatotic liver disease; CMTs: cardiometabolic traits; FDR: false discovery rate; TWAS: transcriptome-wide association study; SMR: Summary-data-based Mendelian Randomization; AAA: abdominal aortic aneurysm; WHRadjBMI: WHR adjusted for BMI; WHR: waist-to-hip ratio; BMI: body mass index; T2D: type 2 diabetes; VTE: venous thromboembolism; TG: triglyceride; nonHDLC: non-HDL cholesterol; MI: myocardial infarction; HyperT: hypertension; CAD: coronary artery disease; HF: heart failure; PAD: peripheral artery disease; AF: atrial fibrillation; FI: fasting insulin.

A comorbidity network for MASLD-CMTs was constructed by compiling the common SNPs and genes, emphasizing the shared variants and genes for each characteristic combination [Figure 5].

Shared genes specific to tissue and cell types

TSEA and CSEA were performed to clarify the influence of shared genes on MASLD-CMTs trait pairs on various tissues and cell types. By integrating these two methodologies, our findings indicate a significant enrichment of liver, adipose, artery, adrenal gland, and brain tissue [Figure 6A], alongside epicardial adipocytes, erythroid progenitor cells, hepatocytes, glial cells, macrophages, monocytes, and myeloid cells [Figure 6B], across numerous MASLD-CMTs trait pairs. Interestingly, brain tissue was enriched only for MASLD and adipose traits, while macrophages and hepatocytes were more linked explicitly to MASLD and lipids. These outcomes generally align with shared genes and biological pathways, consistently focusing on the hepatic-cardiac axis and lipid metabolism.

Single-cell RNA sequencing data analysis

To investigate the cellular mechanisms underlying the co-occurrence of MASLD and CMTs, we carried out a single-cell transcriptomic analysis on liver specimens obtained from Chow and MASH groups. Following quality control, 33,168 cells were identified, with 17,788 from the Chow and 15,380 from the MASH, categorized into eight cell types, including hepatocytes, macrophages, monocytes, fibroblasts, endothelial cells, B cells, T cells, and NK cells [Figure 7A]. The MASH exhibited an increased relative abundance of hepatocytes, macrophages, and monocytes compared to the control, indicating potential involvement of these cell types in the pathogenesis of inflammation and fibrosis associated with MASLD.

Next, we explored the cellular heterogeneity of the shared pathways in patients with MASLD. In MASH, hepatocytes and macrophages were significantly enriched with cholesterol metabolism, glycolysis/gluconeogenesis, PPAR signaling pathway, and long-term depression, which might play a role [Figure 7B and C]. Notably, cholesterol metabolism was significantly enriched in macrophages, exhibiting the highest AUcell score in MASH compared to the Chow [Figure 7D and E]. Glycolysis/Gluconeogenesis was markedly elevated in the MASH, with hepatocytes, macrophages, and monocytes being the primary contributors in comparison to the Chow [Figure 7F]. We also observed that the genes *APOE* and *LPL*, which colocalize with multiple traits within the liver-heart axis, were highly enriched in macrophages and had higher expression levels in the MASH compared to Chow [Figure 7G and H].

Drugs for MASLD with comorbid conditions

A total of 356 disease genes associated with MASLD and different CMTs were identified. Given the frequent coexistence of these disorders, we utilized these genes to identify pharmacological treatments for MASLD with associated comorbidities. In short, we analyzed the pathological pathways for each trait pair through their mutual genes, and mapped the pharmacological pathways for each prospective drug based on the genes they target, as recorded in large-scale drug-gene databases, e.g., DGIdb, DrugCentral, and PharmGKB. Candidate drugs were chiefly obtained by screening cardiometabolic compounds that target the 356 disease genes. Collectively, 48 candidate drugs that target 15 genes in 5 functional categories were examined, namely antihypertensive (26 drugs), anticoagulant (6 drugs), glucose-lowering (5 drugs), lipid-lowering (3 drugs), and other cardiovascular drugs (8 drugs). These drugs have largely been sanctioned for the treatment of a range of cardiometabolic diseases [Figure 8 and Supplementary Table 7]. Since lipid metabolism plays a vital role in the liver-heart axis, we employed a minimum of three gene-level techniques to find more lipid-lowering drugs, leading to the identification of 10 medications [Supplementary Table 8].

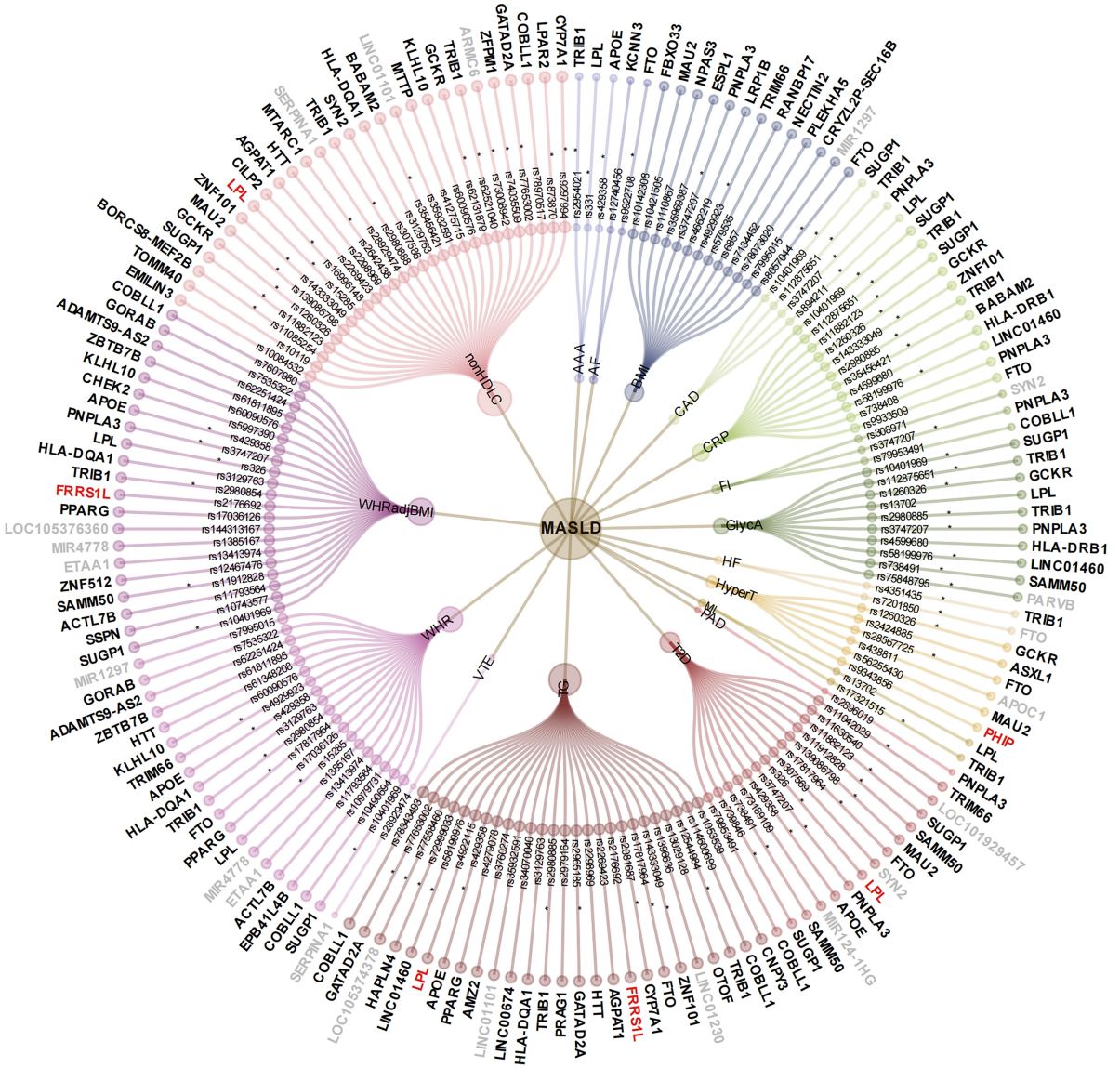

Figure 5. Circular dendrograms display common loci for MASLD and CMTs. Within the inner circle, independent variants shared among MASLD-CMTs trait pairs are shown, with 73 shared causal variants highlighted by asterisks [posterior probability of H4 (PP.H4) > 0.7]. Annovar-inferred genes for the shared variants are depicted in the outer circle. Genes are color-coded to signify their overlap with the four gene recognition methodologies: TWAS, SMR, GCTA-fastBAT, and MAGMA. Gray denotes genes not identified by any approach; black indicates those identified by at least one method, and red represents genes identified by all four methods. MASLD: Metabolic dysfunction-associated steatotic liver disease; CMTs: cardiometabolic traits; TWAS: transcriptome-wide association study; SMR: Summary-data-based Mendelian Randomization; AAA: abdominal aortic aneurysm; WHRadjBMI: WHR adjusted for BMI; WHR: waist-to-hip ratio; BMI: body mass index; T2D: type 2 diabetes; VTE: venous thromboembolism; TG: triglyceride; nonHDLC: non-HDL cholesterol; MI: myocardial infarction; HyperT: hypertension; CAD: coronary artery disease; HF: heart failure; PAD: peripheral artery disease; AF: atrial fibrillation; FI: fasting insulin.

DISCUSSION

Our multi-omics dissection of the liver-heart axis reveals compartment-specific metabolic crosstalk, with hepatic cholesterol dysregulation emerging as a central driver of cardiometabolic comorbidity. A total of 166 loci were discovered to be shared, with the majority linked to cholesterol metabolism, glycolysis, and immune inflammation. We delved deeper into the shared genetic basis, examining potential genes, pathways, tissues, and cell types associated with these trait pairs. Interestingly, scRNA-seq analysis revealed

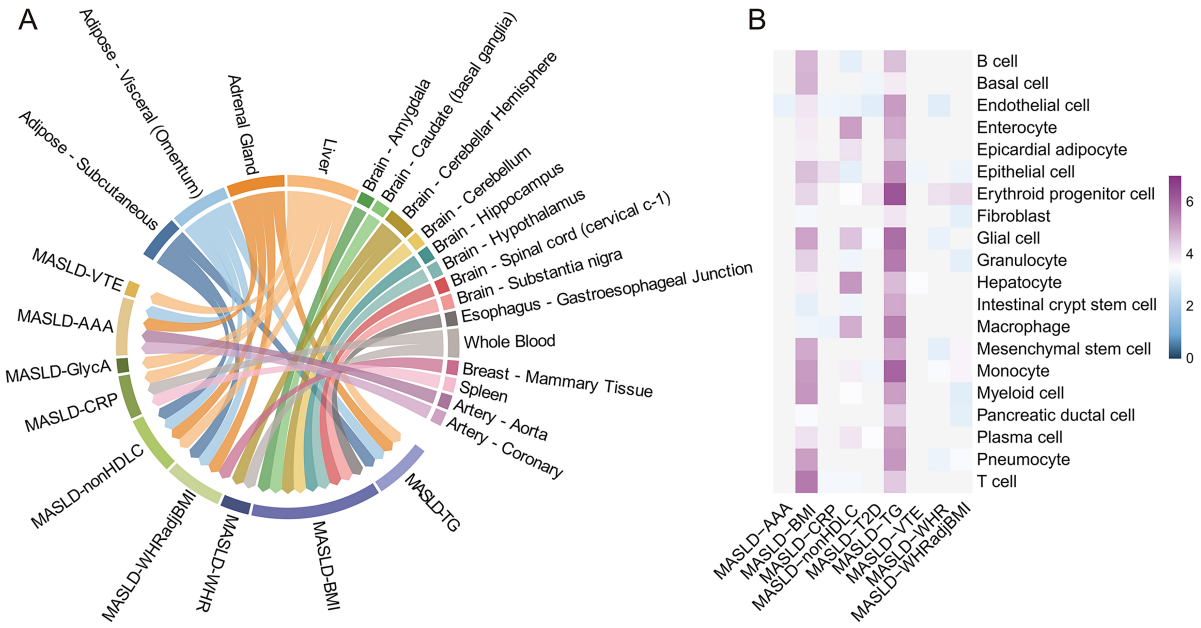

Figure 6. Tissue and cell type specificity derived from the shared signals linking MASLD and CMTs. (A) Tissue enrichment for the shared genes between MASLD and CMTs, as identified by GTEx; (B) Cell type-specific enrichment for the shared genes between MASLD and CMTs, derived from CATLAS or expression of cell type-specific genes in 111 single-cell transcriptomes. MASLD: Metabolic dysfunction-associated steatotic liver disease; CMTs: cardiometabolic traits; GTEx: Genotype-Tissue Expression project; AAA: abdominal aortic aneurysm; WHRadjBMI: WHR adjusted for BMI; WHR: waist-to-hip ratio; BMI: body mass index; T2D: type 2 diabetes; VTE: venous thromboembolism; TG: triglyceride; nonHDLC: non-HDL cholesterol.

a significant upregulation of cholesterol-related genes, particularly *APOE* and *LPL*, in macrophages from MASH patients. These genes demonstrated strong colocalization across multiple trait pairs within the liver-heart axis, highlighting potential mechanisms underlying comorbidities and identifying promising drug targets. Our findings provide new insights into MASLD-CMTs comorbidity and could improve the prediction, diagnosis, and treatment of these conditions.

The liver-heart axis emerges as a bidirectional metabolic amplifier wherein adiposity-driven lipid dysregulation orchestrates multiorgan crosstalk. Consistent with findings from conventional epidemiological studies, we found significant genetic correlations between MASLD and 17 CMTs. For example, we provided strong genetic evidence linking MASLD with adiposity traits, including BMI, WHR, and WHRadjBMI, and MR evidence indicates that those who are obese should be warned about the risk of MASLD. Studies on bariatric surgery revealed that MASLD was present in 85% to 95% of severely obese individuals[54]. Overweight and obese MASLD patients should aim to lose between 7% and 10% of their body weight to significantly reduce liver fat and delay vascular and metabolic complications[55]. We also found a shared genetic mechanism between MASLD and T2D, with MR evidence pointing to a mutual causal relationship. According to a meta-analysis, MASLD frequently co-occurs with T2D, affecting approximately 50% of patients[56]. In alignment with prior research, our findings corroborated the significant genetic correlations between MASLD and various cardiometabolic conditions, including MI[57], HyperT[58], CAD[59], HF[60], PAD[61], VTE[62], AF[63], and AAA[64]. Among nondiabetic patients, the FI levels were significantly higher in patients with MASLD[65,66], suggesting that these levels have diagnostic potential, consistent with our LDSC and MR results. Finally, among all blood pressure traits, only DBP and MASLD showed genetic correlation and causality, indicating that blood pressure abnormalities, particularly DBP, may have potential value for diagnosing MASLD[67-69]. This genetic relationship is further supported by clinical evidence, as a

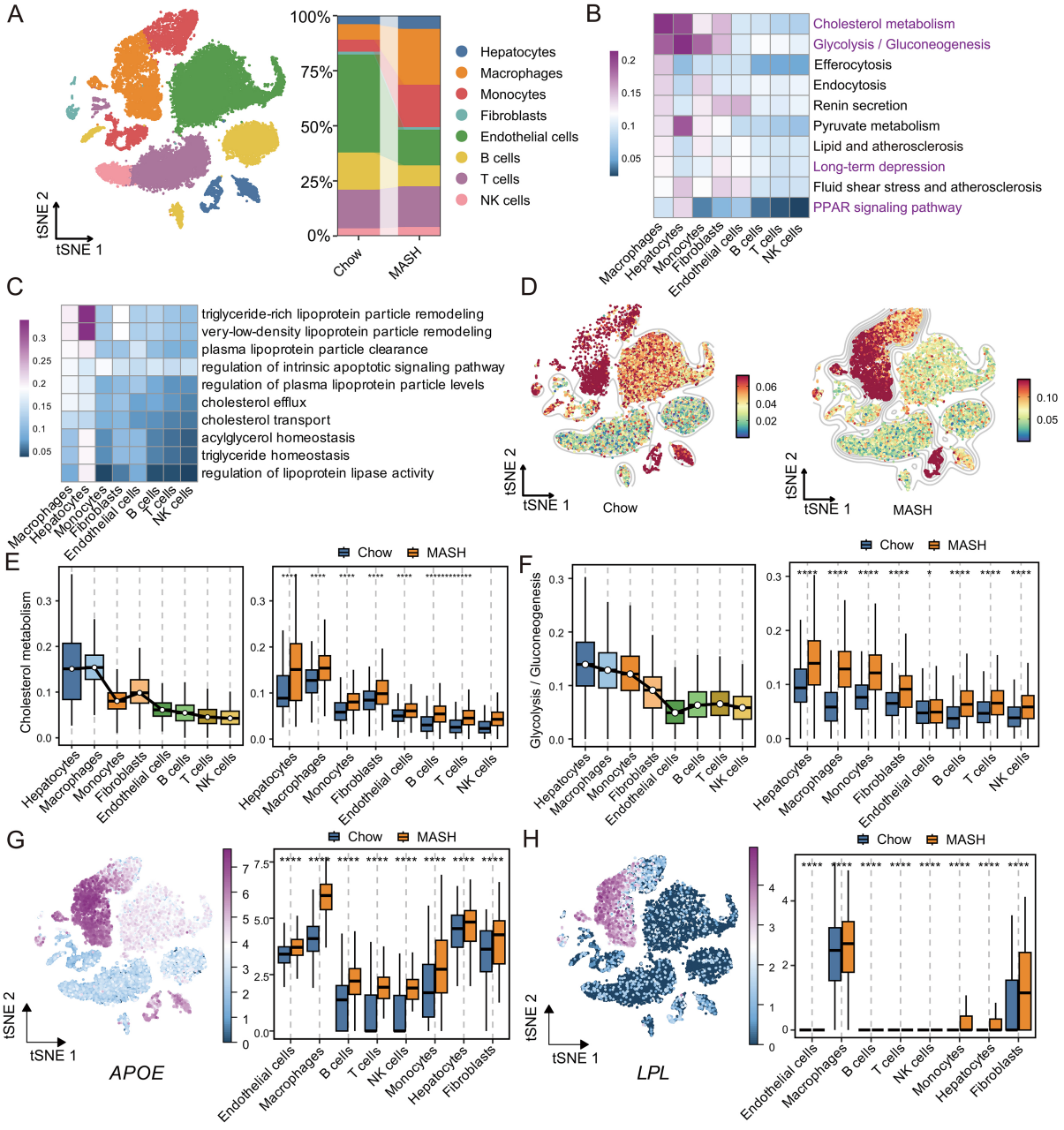

Figure 7. Single-cell RNA sequencing analysis uncovers the shared pathways in MASLD with concurrent conditions. (A) t-SNE and the relative percentage of hepatocytes, macrophages, monocytes, fibroblasts, endothelial cells, B cells, T cells, and NK cells; (B) AUcell scores for the diversity of KEGG pathways across various cell types in MASH; (C) AUcell scores for the diversity of GO pathways across various cell types in MASH; (D) Cholesterol metabolism scores on t-SNE compare Chow (left) and MASH (right), highlighting significant enrichment in macrophages; (E) The cholesterol metabolism score of macrophages in MASH was most significant compared to Chow by the Wilcoxon rank sum test; (F) Glycolysis/gluconeogenesis was significantly increased in MASH, especially in hepatocytes, macrophages, and monocytes, compared to Chow, as shown by the Wilcoxon rank sum test; (G) *APOE* expression was significantly higher in MASH than in Chow, especially in macrophages, as demonstrated by the Wilcoxon rank sum test; (H) *LPL* expression was significantly higher in MASH than in Chow, especially in macrophages, as shown by the Wilcoxon rank sum test. MASLD: Metabolic dysfunction-associated steatotic liver disease; CMTs: cardiometabolic traits; t-SNE: t-distributed Stochastic Neighbor Embedding; GO: gene ontology; MASH; metabolic dysfunction associated steatohepatitis.

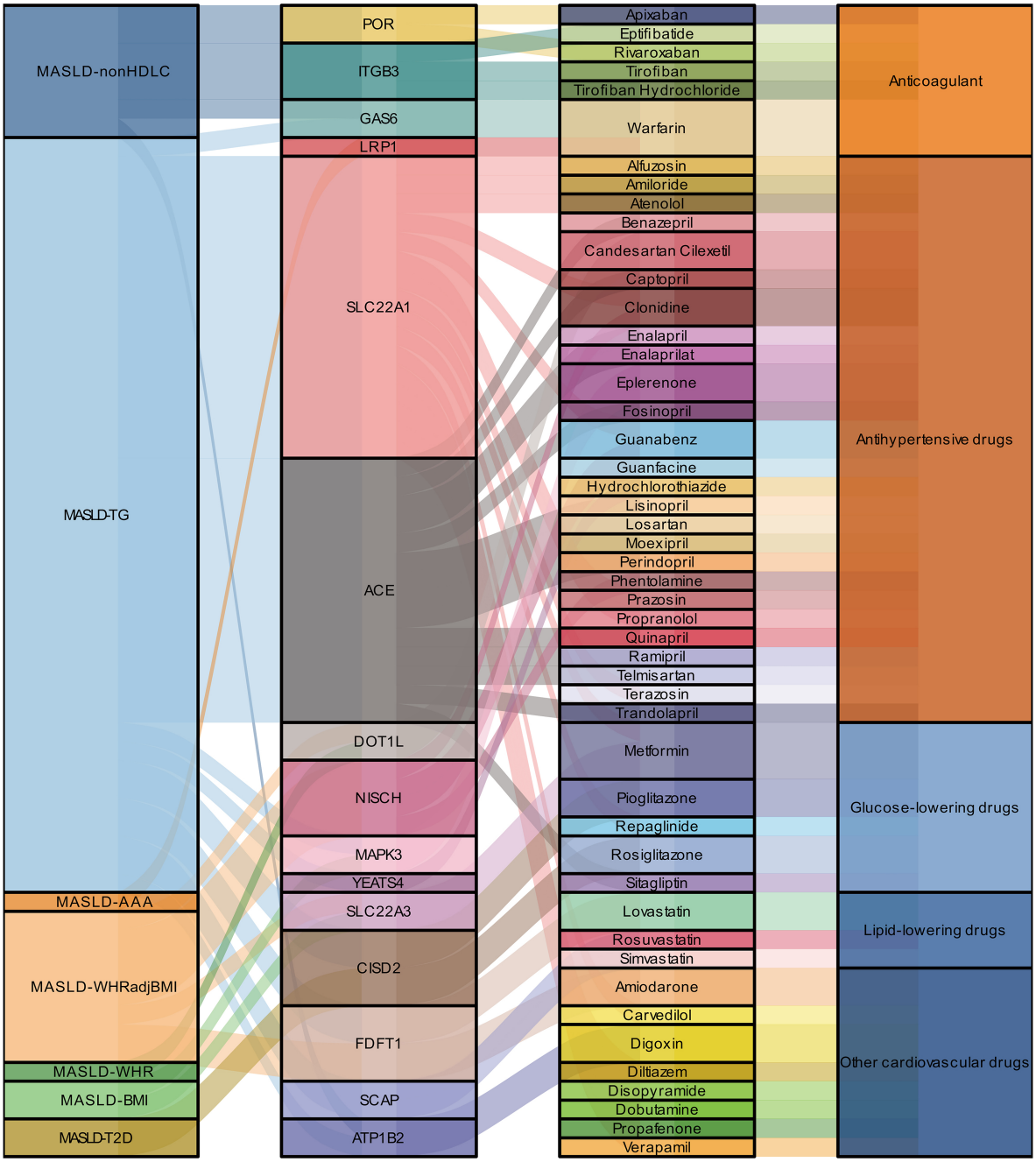

Figure 8. Sankey diagram visualizing the relationships between trait pairs, genes, drugs, and classifications concerning MASLD and cardiometabolic comorbidities. MASLD: Metabolic dysfunction-associated steatotic liver disease; nonHDLC: non-HDL cholesterol; TG: triglyceride; AAA: abdominal aortic aneurysm; WHRadjBMI: WHR adjusted for BMI; WHR: waist-to-hip ratio; BMI: body mass index; T2D: type 2 diabetes.

prospective study found that the risk of incident HyperT increases with the severity of MASLD[70]. Consequently, population-scale longitudinal cohorts with integrated multi-omics platforms are needed for future research to elucidate the dynamic interplay between glycemic variability, blood pressure changes, and MASLD.

A collection of genetic risk loci linking hepatic steatosis to cardiometabolic outcomes in the liver-heart axis was identified, with some appearing in multiple phenotype pairs, such as SNPs located in or near *TRIB1*, *LPL*, *PNPLA3*, *GCKR*, and *PPARG*. Of them, *TRIB1*, specifically rs17321515, was associated with higher serum lipid levels, which could contribute to the development and progression of MASLD and CAD[71-74]. Reinforcing this finding, our study found that *TRIB1* exhibited significant multi-trait colocalization in the liver-heart axis, encompassing MASLD, CAD, MI, nonHDLC, TG, BMI, WHR, WHRadjBMI, and GlycA, thereby emphasizing its pivotal role in linking the liver-heart axis through its potential regulation of lipid metabolism. *LPL*, an enzyme crucial for lipid metabolism, has been implicated in cardiovascular health[75]. Early studies in mice lacking cardiac *LPL* showed that, as they aged, they developed a high incidence of AF, did not respond well to increased afterload, and had over a 50% reduction in HDL-C[76]. Understanding *LPL*'s role in MASLD might assist in formulating targeted therapies to address dyslipidemia and decrease cardiovascular risk. *PNPLA3*, primarily found in the liver and adipose tissue, was crucial for lipid metabolism[77]. In experimental studies, *PNPLA3 148M* led to hepatic steatosis, inflammation, and fibrosis[78]. Conversely, the reduction in *PNPLA3* resulted in a rise in LDL-C and TC, thus increasing the risks of CAD and MI[79]. Addressing *PNPLA3* as a therapeutic target for the treatment of MASLD necessitates a thorough evaluation of its dual function in hepatic and cardiac metabolism, along with careful consideration of the potential metabolic risks to cardiac health. Notably, the *GCKR* rs1260326 genetic variant played a role in impaired liver lipid and glucose metabolism, fostering the onset of metabolic disorders such as MASLD and T2D[80-83]. Modulating *GCKR* could help mitigate the onset and progression of MASLD and cardiometabolic comorbidities by optimizing glucose and lipid metabolism, akin to the effects observed with pioglitazone[84]. As a subtype of the PPAR family, *PPARG* was crucial in regulating lipid metabolism, insulin sensitivity, and inflammation[85,86]. Moreover, our results suggest a causal relationship between MASLD and impaired DBP (as we observed for variants in *CACNB2*[87], *PELI1*[88], *TRIB1*[71], *PNPLA3*[77], *PLCE1*[89,90], and *COBLL1*[91]), which is potentially associated with cardiovascular function, inflammation, and lipid metabolism, thereby highlighting the interaction along the liver-heart axis. Our findings' reliability was enhanced due to the consistent significance of SNPs identified by MTAG in the CPASSOC analysis. Nevertheless, future studies on genetically modified mice (e.g., knock-in/knock-out models) are critical to understanding the role of specific genes and variants, offering new insights into the biological mechanisms of the liver-heart axis.

Lipid metabolism, particularly cholesterol homeostasis, constitutes the molecular linchpin connecting hepatic steatosis and cardiometabolic dysfunction in the liver-heart axis pathophysiological framework. Numerous studies, such as cross-sectional analyses, systematic reviews, and genetic evidence, have shown that MASLD increases the likelihood of developing atherosclerosis and forming unstable plaques, thereby elevating cardiometabolic risk[92-95]. In this study, pathways related to lipid and atherosclerosis, alongside cholesterol metabolism, were significantly enriched, supporting earlier evidence. Across almost all trait pairs, lipid metabolic pathways revealed substantial enrichment, underscoring their central role in MASLD and cardiometabolic comorbidities. Recent research in immunometabolism has demonstrated that changes in the metabolic profile of macrophages, particularly cholesterol metabolism, significantly affect their activation state and functionality, consequently impacting the pathological processes associated with MASLD and cardiometabolic comorbidities[96-98]. Interestingly, our study noted a significant increase in macrophages within the MASH, showing a heightened expression of cholesterol metabolism pathways compared to the Chow, as indicated by scRNA-seq analysis. Prior studies have shown that alterations in hepatic lipid metabolism contribute to dyslipidemia and an elevation in low-density lipoprotein levels, subsequently facilitating foam cell formation and atherogenesis[99,100]. Simultaneously, modifications in liver lipid metabolism were also observed in a mouse model exhibiting hypertrophic cardiomyopathy[101]. Hence, cholesterol metabolism, as a crucial component of lipid metabolism, could be central to the hepatic-cardiac axis, contributing to the comorbidity within the liver-heart axis.

APOE and *LPL* exemplify hepatic-derived genetic amplifiers of cardiometabolic risk, their macrophage-specific dysregulation in MASLD unveiling novel therapeutic targets that modulate the liver-heart axis. Of particular interest is rs429358, located within *APOE*[102], which shows evidence of multi-trait colocalization among MASLD, T2D, WHR, and WHRadjBMI, all implicated in the liver-heart axis. Prior research has shown that increased levels of *APOE* can alter the metabolism of very low-density lipoproteins (VLDL), potentially heightening the risk of atherosclerosis[103]. Building on this, we also identified that *APOE* was significantly enriched and upregulated in macrophages in MASH compared to Chow, suggesting a potential impact on cardiometabolic disease in MASLD patients. Similarly, *LPL*, a gene associated with lipid metabolism and significantly colocalized with multiple trait pairs in the liver-heart axis, such as MASLD with AAA, CAD, and T2D, was markedly upregulated in macrophages during MASH progression. Consequently, lipid-based therapies in the liver-heart axis could be further explored and combined with existing treatments for synergistic clinical benefits.

Beyond lipid-related pathways, other shared pathways between MASLD and CMTs were biologically plausible. Among these was glucose metabolism, involving insulin resistance and the glucagon signaling pathway. MASLD can exacerbate hepatic and systemic insulin resistance and elevate hyperglycemia, subsequently raising the risk of cardiometabolic disease by facilitating monocyte/macrophage adhesion to the endothelium, promoting vascular smooth muscle cell proliferation and causing endothelial dysfunction[104-106]. Our scRNA-seq analysis showed a notable increase in glycolysis/gluconeogenesis in various cells in MASH compared to Chow, including hepatocytes, macrophages, and monocytes. The PPAR signaling pathway, also identified in our study, was involved in glucose and lipid metabolism across various organs[107-109] and impacted macrophage polarization[110,111], thereby influencing the liver-heart axis microenvironment. Lastly, ER stress, which could trigger cellular senescence[112], has a notable effect on the impairment of insulin signaling[113], which was linked to the development of diabetes and the progression of MASLD to MASH[114,115]. Overall, multiple mechanisms interacting synergistically resulted in MASLD and cardiometabolic comorbidities.

Our multi-omics dissection uncovers macrophage-driven neuroimmunometabolic crosstalk in the cardio-cerebral-hepatic axis, where long-term depression pathway dysregulation underlies the metabo-psychiatric comorbidities observed in MASLD progression. Specifically, our findings showed that when brain tissues, especially the amygdala, a crucial center for socioemotional and cognitive functions[116], exhibited a significant association with MASLD and obesity traits, the long-term depression pathway was significantly enriched in macrophages during MASH. Prior investigations have shown that depression was more prevalent among patients suffering from MASLD and cardiometabolic disorders[117-120]. MASLD is linked to diminished cognitive function and influences different kinds of memory[121], where the metabolic disruptions reflect a mismatch between lipid-clearing and lipid-increasing mechanisms. This imbalance might be attributed to the shared risk factors, including obesity, dyslipidemia, and immune response in cardio-cerebral-hepatic axis diseases[122-124], collectively underscoring the need for further study through extensive clinical trials and animal research. Based on these findings, we recommend that clinicians monitor the emotional well-being of patients with MASLD and concurrent cardiometabolic disorders, with psychotherapy explored as an adjunct to pharmacological treatments.

A single treatment is unlikely to reverse liver fibrosis or enhance the cardiometabolic microenvironment across all patients. Moving forward, personalized therapies and drug combinations are expected to gain preference. Numerous medications, such as antihypertensive, anticoagulant, glucose-lowering, lipid-lowering, and other cardiovascular drugs, have shown potential in treating MASLD and its comorbidities. Most drug candidates identified in our study are already in use for cardiometabolic conditions, with some,

such as metformin[125,126] and pioglitazone[127,128], undergoing clinical trials for repurposing to target MASLD. However, the efficacy of these pharmacological interventions for such comorbidities remains inconclusive. Further clinical research is essential to evaluate their therapeutic effectiveness. Thus, they ought to be employed judiciously in clinical decision making. In parallel, combating MASLD and its associated cardiometabolic risks should prioritize promoting healthy lifestyles, improving nutritional literacy, and encouraging smoking cessation[129].

Our study's primary strengths lie in integrating triangulated evidence from GWAS and scRNA-seq techniques to uncover the common genetic foundation and biological mechanisms of MASLD and CMTs. To ensure high statistical power, we included a substantial number of GWAS with sample sizes ranging from 115,078 to 1,996,991 individuals and enhanced this power through sensitivity analyses. Additionally, investigating a wide variety of CMTs enabled a comprehensive examination of the shared mechanisms between different cardiometabolic comorbidities and MASLD. To minimize the risk of type I statistical errors, we applied strict FDR correction and integrated frequentist approaches with multi-trait colocalization, thereby enhancing our confidence in the results.

Several limitations need to be acknowledged. Since the GWAS data were derived mainly from European ancestry, the generalizability of our conclusions is limited. Future studies should include a broader range of ancestries. According to previous research, hepatic steatosis and cardiovascular disease might be related differently across genders[130]. Employing sex-specific GWAS data could thus prove beneficial for future research by elucidating these differences. While MASLD accounts for most fatty liver disease cases, replicating our study in metabolic and alcohol-associated/accompanying liver disease (MetALD)[131] could enhance our understanding of cardiometabolic risks across different liver disease subtypes, thereby aiding precise diagnosis and personalized treatment. Finally, this study gathered scRNA-seq data from samples related to MASH and Chow. However, it did not include sequencing data on the coexistence of MASH with cardiometabolic disorders, which restricted the analysis of potential interactions in the hepatic-cardiac axis. Incorporating additional RNA sequencing data on various MASLD and cardiometabolic comorbidities could provide even deeper insights into these interactions.

This study provides a multifaceted understanding of the association between MASLD and CMTs, offering a comprehensive and reliable map of liver-heart axis interactions. Our findings confirm and expand upon prior knowledge. While providing robust genetic evidence for the relationship between MASLD and CMTs, we further explored their underlying mechanisms of association, specifically identifying shared variants, genes, pathways, cell types, and tissues. The link between MASLD and cardiometabolic disorders involves multiple biological pathways and is likely influenced significantly by lipid regulation. These distinctive insights underscore the critical role of the liver-heart axis and suggest potential implications for clinical practice, indicating the need for more tailored therapeutic strategies that prioritize cardiometabolic disorders in patients with MASLD. These patients represent a high-risk population, including those with conditions such as obesity, diabetes, and HyperT.

DECLARATIONS

Acknowledgments

The authors acknowledge the contributions of those researchers who produced and disseminated the genetic and scRNA-seq datasets employed in this investigation. Additionally, the authors appreciate the support provided by Figdraw (https://www.figdraw.com/).

Authors' contributions

Worked together to design the study: Wang XY, Lyu Q, Xie YY
Conducted the main analyses: Wang XY
Assisted in drug prediction: Lyu Q
Offered essential biological perspectives for understanding the results: Wang XY, Lyu Q, Zhang YY, Su Y, Zhao H, Shen HH, Xie YY
Drafted the manuscript: Wang XY
All authors critically reviewed the manuscript.

Availability of data and materials

Supplementary Table 1 contains the GWAS summary statistics for this study. GTEx provided the eQTL summary data for several tissues. Single-cell RNA sequencing data for non-parenchymal cells in healthy and MASH mouse livers were retrieved from GEO under accession code GSE129516. Other raw data that support the findings of this study are available from the corresponding author upon reasonable request.

Financial support and sponsorship

This study was supported by the National Natural Science Foundation of China (No.82104721).

Conflicts of interest

All authors declared that there are no conflicts of interest.

Ethical approval and consent to participate

Not applicable.

Consent for publication

Not applicable.

REFERENCES

1. Haas JT, Francque S, Staels B. Pathophysiology and mechanisms of nonalcoholic fatty liver disease. *Annu Rev Physiol.* 2016;78:181-205. DOI PubMed
2. Lonardo A, Byrne CD, Caldwell SH, Cortez-Pinto H, Targher G. Global epidemiology of nonalcoholic fatty liver disease: meta-analytic assessment of prevalence, incidence, and outcomes. *Hepatology.* 2016;64:1388-9. DOI PubMed
3. Shang Y, Nasr P, Widman L, Hagström H. Risk of cardiovascular disease and loss in life expectancy in NAFLD. *Hepatology.* 2022;76:1495-505. DOI PubMed PMC
4. Foley CN, Staley JR, Breen PG, et al. A fast and efficient colocalization algorithm for identifying shared genetic risk factors across multiple traits. *Nat Commun.* 2021;12:764. DOI PubMed PMC
5. Li P, Ji H, Cheng S. Heart-liver axis implications of the new steatotic liver disease nomenclature. *Lancet Gastroenterol Hepatol.* 2023;8:1071-2. DOI PubMed
6. Baskin KK, Bookout AL, Olson EN. The heart-liver metabolic axis: defective communication exacerbates disease. *EMBO Mol Med.* 2014;6:436-8. DOI PubMed PMC
7. Zhou J, Bai L, Zhang XJ, Li H, Cai J. Nonalcoholic fatty liver disease and cardiac remodeling risk: pathophysiological mechanisms and clinical implications. *Hepatology.* 2021;74:2839-47. DOI PubMed
8. Mantovani A, Csermely A, Petracca G, et al. Non-alcoholic fatty liver disease and risk of fatal and non-fatal cardiovascular events: an updated systematic review and meta-analysis. *Lancet Gastroenterol Hepatol.* 2021;6:903-13. DOI PubMed
9. Simon TG, Roelstraete B, Hagström H, Sundström J, Ludvigsson JF. Non-alcoholic fatty liver disease and incident major adverse cardiovascular events: results from a nationwide histology cohort. *Gut.* 2022;71:1867-75. DOI PubMed
10. Younossi ZM, Paik JM, Stepanova M, Ong J, Alqahtani S, Henry L. Clinical profiles and mortality rates are similar for metabolic dysfunction-associated steatotic liver disease and non-alcoholic fatty liver disease. *J Hepatol.* 2024;80:694-701. DOI PubMed
11. Oh JH, Jun DW. Clinical impact of five cardiometabolic risk factors in metabolic dysfunction-associated steatotic liver disease

(MASLD): insights into regional and ethnic differences. *Clin Mol Hepatol.* 2024;30:168-70. DOI PubMed PMC
12. Rinella ME, Neuschwander-Tetri BA, Siddiqui MS, et al. AASLD practice guidance on the clinical assessment and management of nonalcoholic fatty liver disease. *Hepatology.* 2023;77:1797-835. DOI PubMed PMC
13. Abdelhameed F, Kite C, Lagojda L, et al. Non-invasive scores and serum biomarkers for fatty liver in the era of metabolic dysfunction-associated steatotic liver disease (MASLD): a comprehensive review from NAFLD to MAFLD and MASLD. *Curr Obes Rep.* 2024;13:510-31. DOI PubMed PMC
14. Isaak A, Praktiknjo M, Jansen C, et al. Myocardial fibrosis and inflammation in liver cirrhosis: MRI study of the liver-heart axis. *Radiology.* 2020;297:51-61. DOI PubMed
15. Burelle C, Clapatiuc V, Deschênes S, et al. A genetic mouse model of lean-NAFLD unveils sexual dimorphism in the liver-heart axis. *Commun Biol.* 2024;7:356. DOI PubMed PMC
16. Anstee QM, Darlay R, Cockell S, et al; EPoS Consortium Investigators. Genome-wide association study of non-alcoholic fatty liver and steatohepatitis in a histologically characterised cohort☆. *J Hepatol.* 2020;73:505-15. DOI PubMed
17. Claussnitzer M, Cho JH, Collins R, et al. A brief history of human disease genetics. *Nature.* 2020;577:179-89. DOI PubMed PMC
18. Sonehara K, Okada Y. Leveraging genome-wide association studies to better understand the etiology of cancers. *Cancer Sci.* 2025;116:288-96. DOI PubMed PMC
19. Lau PP, Wei CY, Lin MR, Chou WH, Wan YY, Chang WC. Genome-wide association study of the fatty liver index in the Taiwanese population reveals shared and population-specific genetic risk factors across ethnicities. *Cell Biosci.* 2025;15:19. DOI PubMed PMC
20. Torgersen K, Rahman Z, Bahrami S, et al. Shared genetic loci between depression and cardiometabolic traits. *PLoS Genet.* 2022;18:e1010161. DOI PubMed PMC
21. Trépo E, Valenti L. Update on NAFLD genetics: from new variants to the clinic. *J Hepatol.* 2020;72:1196-209. DOI PubMed
22. Eslam M, George J. Genetic contributions to NAFLD: leveraging shared genetics to uncover systems biology. *Nat Rev Gastroenterol Hepatol.* 2020;17:40-52. DOI PubMed
23. Hong X, Wu Z, Cao W, et al. Cardiometabolic traits in adult twins: heritability and BMI impact with age. *Nutrients.* 2022;15:164. DOI PubMed PMC
24. Ghodsian N, Abner E, Emdin CA, et al. Electronic health record-based genome-wide meta-analysis provides insights on the genetic architecture of non-alcoholic fatty liver disease. *Cell Rep Med.* 2021;2:100437. DOI PubMed PMC
25. Bulik-Sullivan B, Finucane HK, Anttila V, et al; ReproGen Consortium, Psychiatric Genomics Consortium, Genetic Consortium for Anorexia Nervosa of the Wellcome Trust Case Control Consortium 3. An atlas of genetic correlations across human diseases and traits. *Nat Genet.* 2015;47:1236-41. DOI
26. Burgess S, Butterworth A, Thompson SG. Mendelian randomization analysis with multiple genetic variants using summarized data. *Genet Epidemiol.* 2013;37:658-65. DOI PubMed PMC
27. Burgess S, Thompson SG. Interpreting findings from Mendelian randomization using the MR-Egger method. *Eur J Epidemiol.* 2017;32:377-89. DOI PubMed PMC
28. Bowden J, Davey Smith G, Haycock PC, Burgess S. Consistent estimation in Mendelian randomization with some invalid instruments using a weighted median estimator. *Genet Epidemiol.* 2016;40:304-14. DOI PubMed PMC
29. Hu X, Zhao J, Lin Z, et al. Mendelian randomization for causal inference accounting for pleiotropy and sample structure using genome-wide summary statistics. *Proc Natl Acad Sci U S A.* 2022;119:e2106858119. DOI PubMed PMC
30. Purcell S, Neale B, Todd-Brown K, et al. PLINK: a tool set for whole-genome association and population-based linkage analyses. *Am J Hum Genet.* 2007;81:559-75. DOI PubMed PMC
31. Hemani G, Zheng J, Elsworth B, et al. The MR-Base platform supports systematic causal inference across the human phenome. *Elife.* 2018;7:e34408. DOI PubMed PMC
32. O'Connor LJ, Price AL. Distinguishing genetic correlation from causation across 52 diseases and complex traits. *Nat Genet.* 2018;50:1728-34. DOI PubMed PMC
33. Turley P, Walters RK, Maghzian O, et al; 23andMe Research Team, Social Science Genetic Association Consortium. Multi-trait analysis of genome-wide association summary statistics using MTAG. *Nat Genet.* 2018;50:229-37. DOI PubMed PMC
34. Zhu X, Feng T, Tayo BO, et al; COGENT BP Consortium. Meta-analysis of correlated traits via summary statistics from GWASs with an application in hypertension. *Am J Hum Genet.* 2015;96:21-36. DOI PubMed PMC
35. Wang K, Li M, Hakonarson H. ANNOVAR: functional annotation of genetic variants from high-throughput sequencing data. *Nucleic Acids Res.* 2010;38:e164. DOI PubMed PMC
36. Wallace C. Statistical testing of shared genetic control for potentially related traits. *Genet Epidemiol.* 2013;37:802-13. DOI PubMed PMC
37. Gusev A, Ko A, Shi H, et al. Integrative approaches for large-scale transcriptome-wide association studies. *Nat Genet.* 2016;48:245-52. DOI PubMed PMC
38. Zhu Z, Zhang F, Hu H, et al. Integration of summary data from GWAS and eQTL studies predicts complex trait gene targets. *Nat Genet.* 2016;48:481-7. DOI PubMed
39. Bakshi A, Zhu Z, Vinkhuyzen AA, et al. Fast set-based association analysis using summary data from GWAS identifies novel gene loci for human complex traits. *Sci Rep.* 2016;6:32894. DOI PubMed PMC
40. de Leeuw CA, Mooij JM, Heskes T, Posthuma D. MAGMA: generalized gene-set analysis of GWAS data. *PLoS Comput Biol.*

2015;11:e1004219. DOI PubMed PMC
41. Consortium. The GTEx consortium atlas of genetic regulatory effects across human tissues. *Science*. 2020;369:1318-30. DOI PubMed PMC
42. Feng H, Mancuso N, Gusev A, et al. Leveraging expression from multiple tissues using sparse canonical correlation analysis and aggregate tests improves the power of transcriptome-wide association studies. *PLoS Genet.* 2021;17:e1008973. DOI PubMed PMC
43. Xu S, Hu E, Cai Y, et al. Using clusterProfiler to characterize multiomics data. *Nat Protoc.* 2024;19:3292-320. DOI PubMed
44. Dougherty JD, Schmidt EF, Nakajima M, Heintz N. Analytical approaches to RNA profiling data for the identification of genes enriched in specific cells. *Nucleic Acids Res.* 2010;38:4218-30. DOI PubMed PMC
45. Dai Y, Hu R, Liu A, et al. WebCSEA: web-based cell-type-specific enrichment analysis of genes. *Nucleic Acids Res.* 2022;50:W782-90. DOI PubMed PMC
46. Xiong X, Kuang H, Ansari S, et al. Landscape of intercellular crosstalk in healthy and NASH liver revealed by single-cell secretome gene analysis. *Mol Cell.* 2019;75:644-60.e5. DOI PubMed PMC
47. Stuart T, Butler A, Hoffman P, et al. Comprehensive integration of single-cell data. *Cell.* 2019;177:1888-902.e21. DOI PubMed PMC
48. Korsunsky I, Millard N, Fan J, et al. Fast, sensitive and accurate integration of single-cell data with harmony. *Nat Methods.* 2019;16:1289-96. DOI PubMed PMC
49. Aran D, Looney AP, Liu L, et al. Reference-based analysis of lung single-cell sequencing reveals a transitional profibrotic macrophage. *Nat Immunol.* 2019;20:163-72. DOI PubMed PMC
50. Saul D, Kosinsky RL, Atkinson EJ, et al. A new gene set identifies senescent cells and predicts senescence-associated pathways across tissues. *Nat Commun.* 2022;13:4827. DOI PubMed PMC
51. Cotto KC, Wagner AH, Feng YY, et al. DGIdb 3.0: a redesign and expansion of the drug-gene interaction database. *Nucleic Acids Res.* 2018;46:D1068-73. DOI PubMed PMC
52. Ursu O, Holmes J, Bologa CG, et al. DrugCentral 2018: an update. *Nucleic Acids Res.* 2019;47:D963-70. DOI PubMed PMC
53. Barbarino JM, Whirl-Carrillo M, Altman RB, Klein TE. PharmGKB: a worldwide resource for pharmacogenomic information. *Wiley Interdiscip Rev Syst Biol Med.* 2018;10:e1417. DOI PubMed PMC
54. Mathews SE, Kumar RB, Shukla AP. Nonalcoholic steatohepatitis, obesity, and cardiac dysfunction. *Curr Opin Endocrinol Diabetes Obes.* 2018;25:315-20. DOI PubMed
55. Niederseer D, Wernly B, Aigner E, Stickel F, Datz C. NAFLD and cardiovascular diseases: epidemiological, mechanistic and therapeutic considerations. *J Clin Med.* 2021;10:467. DOI PubMed PMC
56. Younossi ZM, Golabi P, de Avila L, et al. The global epidemiology of NAFLD and NASH in patients with type 2 diabetes: a systematic review and meta-analysis. *J Hepatol.* 2019;71:793-801. DOI PubMed
57. Xie W, Gan J, Zhou X, et al. Myocardial infarction accelerates the progression of MASH by triggering immunoinflammatory response and induction of periosti. *Cell Metab.* 2024;36:1269-86.e9. DOI PubMed
58. Zhao YC, Zhao GJ, Chen Z, She ZG, Cai J, Li H. Nonalcoholic fatty liver disease: an emerging driver of hypertension. *Hypertension.* 2020;75:275-84. DOI PubMed
59. Ren Z, Simons PIHG, Wesselius A, Stehouwer CDA, Brouwers MCGJ. Relationship between NAFLD and coronary artery disease: a Mendelian randomization study. *Hepatology.* 2023;77:230-8. DOI PubMed PMC
60. Park J, Kim G, Kim H, Lee J, Jin SM, Kim JH. The associations between changes in hepatic steatosis and heart failure and mortality: a nationwide cohort study. *Cardiovasc Diabetol.* 2022;21:287. DOI PubMed PMC
61. Liu Y, Wang J, Jin R, et al. Associations of metabolic dysfunction-associated fatty liver disease with peripheral artery disease: prospective analysis in the UK biobank and ARIC study. *J Am Heart Assoc.* 2024;13:e035265. DOI PubMed PMC
62. Pandey N, Anand SK, Kaur H, et al. Enhanced venous thrombosis and hypercoagulability in murine and human metabolic dysfunction-associated steatohepatitis. *J Thromb Haemost.* 2024;22:3572-80. DOI PubMed PMC
63. Cho EJ, Chung GE, Yoo JJ, et al. Association of nonalcoholic fatty liver disease with new-onset atrial fibrillation stratified by age groups. *Cardiovasc Diabetol.* 2024;23:340. DOI PubMed PMC
64. Jia Y, Li Y, Yu J, et al. Association between metabolic dysfunction-associated fatty liver disease and abdominal aortic aneurysm. *Nutr Metab Cardiovasc Dis.* 2024;34:953-62. DOI PubMed
65. Bril F, McPhaul MJ, Kalavalapalli S, et al. Intact fasting insulin identifies nonalcoholic fatty liver disease in patients without diabetes. *J Clin Endocrinol Metab.* 2021;106:e4360-71. DOI PubMed
66. Pang Y, Kartsonaki C, Turnbull I, et al. Diabetes, plasma glucose, and incidence of fatty liver, cirrhosis, and liver cancer: a prospective study of 0.5 million people. *Hepatology.* 2018;68:1308-18. DOI PubMed PMC
67. Hu Y, Tang W, Liu Y, et al. Temporal relationship between hepatic steatosis and blood pressure elevation and the mediation effect in the development of cardiovascular disease. *Hypertens Res.* 2024;47:1811-21. DOI PubMed
68. Yuan M, He J, Hu X, et al. Hypertension and NAFLD risk: insights from the NHANES 2017-2018 and Mendelian randomization analyses. *Chin Med J.* 2024;137:457-64. DOI PubMed PMC
69. Ciardullo S, Monti T, Sala I, Grassi G, Mancia G, Perseghin G. Nonalcoholic fatty liver disease and advanced fibrosis in US adults across blood pressure categories. *Hypertension.* 2020;76:562-8. DOI PubMed
70. Song Q, Ling Q, Fan L, et al. Severity of non-alcoholic fatty liver disease is a risk factor for developing hypertension from prehypertension. *Chin Med J.* 2023;136:1591-7. DOI PubMed PMC

71. Iwamoto S, Boonvisut S, Makishima S, Ishizuka Y, Watanabe K, Nakayama K. The role of TRIB1 in lipid metabolism; from genetics to pathways. *Biochem Soc Trans*. 2015;43:1063-8. DOI PubMed
72. Functional analysis of the TRIB1 associated locus linked to plasma triglycerides and coronary artery disease. *J Am Heart Assoc*. 2016;5:e002056. DOI PubMed PMC
73. Kitamoto A, Kitamoto T, Nakamura T, et al. Association of polymorphisms in GCKR and TRIB1 with nonalcoholic fatty liver disease and metabolic syndrome traits. *Endocr J*. 2014;61:683-9. DOI PubMed
74. Liu Q, Xue F, Meng J, et al. TRIB1 rs17321515 and rs2954029 gene polymorphisms increase the risk of non-alcoholic fatty liver disease in Chinese Han population. *Lipids Health Dis*. 2019;18:61. DOI PubMed PMC
75. Wang H, Eckel RH. Lipoprotein lipase: from gene to obesity. *Am J Physiol Endocrinol Metab*. 2009;297:E271-88. DOI PubMed
76. Goldberg IJ. 2017 George Lyman Duff memorial lecture: fat in the blood, fat in the artery, fat in the heart: triglyceride in physiology and disease. *Arterioscler Thromb Vasc Biol*. 2018;38:700-6. DOI PubMed PMC
77. Chalasani N, Vilar-Gomez E, Loomba R, et al. PNPLA3 rs738409, age, diabetes, sex, and advanced fibrosis jointly contribute to the risk of major adverse liver outcomes in metabolic dysfunction-associated steatotic liver disease. *Hepatology*. 2024;80:1212-26. DOI PubMed PMC
78. Bruschi FV, Tardelli M, Herac M, Claudel T, Trauner M. Metabolic regulation of hepatic PNPLA3 expression and severity of liver fibrosis in patients with NASH. *Liver Int*. 2020;40:1098-110. DOI PubMed PMC
79. Zhang G, Jiang W, He F, et al. LDL-C and TC mediate the risk of PNPLA3 inhibition in cardiovascular diseases. *J Clin Endocrinol Metab*. 2025;110:e231-8. DOI PubMed
80. Chen G, Shriner D, Zhang J, et al. Additive genetic effect of *GCKR*, *G6PC2*, and *SLC30A8* variants on fasting glucose levels and risk of type 2 diabetes. *PLoS One*. 2022;17:e0269378. DOI PubMed PMC
81. Vaxillaire M, Cavalcanti-Proença C, Dechaume A, et al; DESIR Study Group. The common P446L polymorphism in GCKR inversely modulates fasting glucose and triglyceride levels and reduces type 2 diabetes risk in the DESIR prospective general French population. *Diabetes*. 2008;57:2253-7. DOI PubMed PMC
82. Socha P, Wierzbicka A, Neuhoff-Murawska J, Wlodarek D, Podlesny J, Socha J. Nonalcoholic fatty liver disease as a feature of the metabolic syndrome. *Rocz Panstw Zakl Hig*. 2007;58:129-37. PubMed
83. Petit JM, Masson D, Guiu B, et al. GCKR polymorphism influences liver fat content in patients with type 2 diabetes. *Acta Diabetol*. 2016;53:237-42. DOI PubMed
84. Brouwers MCGJ, Simons N, Stehouwer CDA, Isaacs A. Non-alcoholic fatty liver disease and cardiovascular disease: assessing the evidence for causality. *Diabetologia*. 2020;63:253-60. DOI PubMed PMC
85. Ll, Siersbæk M, Mandrup S. PPARs: fatty acid sensors controlling metabolism. *Semin Cell Dev Biol*. 2012;23:631-9. DOI PubMed
86. Qiu YY, Zhang J, Zeng FY, Zhu YZ. Roles of the peroxisome proliferator-activated receptors (PPARs) in the pathogenesis of nonalcoholic fatty liver disease (NAFLD). *Pharmacol Res*. 2023;192:106786. DOI PubMed
87. El Cheikh J, Hamed F, Rifi H, Dakroub AH, Eid AH. Genetic polymorphisms influencing antihypertensive drug responses. *Br J Pharmacol*. 2025;182:929-50. DOI PubMed
88. Du Y, Wu L, Wang L, Reiter RJ, Lip GYH, Ren J. Extracellular vesicles in cardiovascular diseases: from pathophysiology to diagnosis and therapy. *Cytokine Growth Factor Rev*. 2023;74:40-55. DOI PubMed
89. Li W, Li Y, Chu Y, et al. PLCE1 promotes myocardial ischemia-reperfusion injury in H/R H9c2 cells and I/R rats by promoting inflammation. *Biosci Rep*. 2019;39:BSR20181613. DOI PubMed PMC
90. Evangelou E, Warren HR, Mosen-Ansorena D, et al; Million Veteran Program. Genetic analysis of over 1 million people identifies 535 new loci associated with blood pressure traits. *Nat Genet*. 2018;50:1412-25. DOI PubMed PMC
91. DeForest N, Wang Y, Zhu Z, et al. Genome-wide discovery and integrative genomic characterization of insulin resistance loci using serum triglycerides to HDL-cholesterol ratio as a proxy. *Nat Commun*. 2024;15:8068. DOI PubMed PMC
92. Deprince A, Haas JT, Staels B. Dysregulated lipid metabolism links NAFLD to cardiovascular disease. *Mol Metab*. 2020;42:101092. DOI PubMed PMC
93. Castillo-Leon E, Connelly MA, Konomi JV, Caltharp S, Cleeton R, Vos MB. Increased atherogenic lipoprotein profile in children with non-alcoholic steatohepatitis. *Pediatr Obes*. 2020;15:e12648. DOI PubMed
94. Nass KJ, van den Berg EH, Faber KN, Schreuder TCMA, Blokzijl H, Dullaart RPF. High prevalence of apolipoprotein B dyslipoproteinemias in non-alcoholic fatty liver disease: the lifelines cohort study. *Metabolism*. 2017;72:37-46. DOI PubMed
95. Chandrasekharan K, Alazawi W. Genetics of non-alcoholic fatty liver and cardiovascular disease: implications for therapy? *Front Pharmacol*. 2020;10:1413. DOI PubMed PMC
96. Widjaja AA, Singh BK, Adami E, et al. Inhibiting interleukin 11 signaling reduces hepatocyte death and liver fibrosis, inflammation, and steatosis in mouse models of nonalcoholic steatohepatitis. *Gastroenterology*. 2019;157:777-92.e14. DOI PubMed
97. Vos DY, van de Sluis B. Function of the endolysosomal network in cholesterol homeostasis and metabolic-associated fatty liver disease (MAFLD). *Mol Metab*. 2021;50:101146. DOI PubMed PMC
98. Yu Y, Liu Y, An W, Song J, Zhang Y, Zhao X. STING-mediated inflammation in Kupffer cells contributes to progression of nonalcoholic steatohepatitis. *J Clin Invest*. 2019;129:546-55. DOI PubMed PMC
99. Jaitin DA, Adlung L, Thaiss CA, et al. Lipid-associated macrophages control metabolic homeostasis in a Trem2-dependent manner. *Cell*. 2019;178:686-98.e14. DOI PubMed PMC
100. Cochain C, Vafadarnejad E, Arampatzi P, et al. Single-cell RNA-Seq reveals the transcriptional landscape and heterogeneity of aortic

macrophages in murine atherosclerosis. *Circ Res*. 2018;122:1661-74. DOI PubMed

101. Magida JA, Leinwand LA. Metabolic crosstalk between the heart and liver impacts familial hypertrophic cardiomyopathy. *EMBO Mol Med*. 2014;6:482-95. DOI PubMed PMC
102. Jamialahmadi O, Mancina RM, Ciociola E, et al. Exome-wide association study on alanine aminotransferase identifies sequence variants in the GPAM and APOE associated with fatty liver disease. *Gastroenterology*. 2021;160:1634-46.e7. DOI PubMed
103. van den Berg EH, Corsetti JP, Bakker SJL, Dullaart RPF. Plasma ApoE elevations are associated with NAFLD: the PREVEND study. *PLoS One*. 2019;14:e0220659. DOI PubMed PMC
104. Byrne CD, Targher G. Non-alcoholic fatty liver disease-related risk of cardiovascular disease and other cardiac complications. *Diabetes Obes Metab*. 2022;24:28-43. DOI PubMed
105. Caussy C, Aubin A, Loomba R. The relationship between type 2 diabetes, NAFLD, and cardiovascular risk. *Curr Diab Rep*. 2021;21:15. DOI PubMed PMC
106. Armandi A, Rosso C, Caviglia GP, Bugianesi E. Insulin resistance across the spectrum of nonalcoholic fatty liver disease. *Metabolites*. 2021;11:155. DOI PubMed PMC
107. Matsusue K, Haluzik M, Lambert G, et al. Liver-specific disruption of PPARgamma in leptin-deficient mice improves fatty liver but aggravates diabetic phenotypes. *J Clin Invest*. 2003;111:737-47. DOI PubMed PMC
108. Brocker CN, Patel DP, Velenosi TJ, et al. Extrahepatic PPARα modulates fatty acid oxidation and attenuates fasting-induced hepatosteatosis in mice. *J Lipid Res*. 2018;59:2140-52. DOI PubMed PMC
109. Sanderson LM, Boekschoten MV, Desvergne B, Müller M, Kersten S. Transcriptional profiling reveals divergent roles of PPARα and PPARβ/δ in regulation of gene expression in mouse liver. *Physiol Genomics*. 2010;41:42-52. DOI PubMed
110. Odegaard JI, Ricardo-Gonzalez RR, Red Eagle A, et al. Alternative M2 activation of Kupffer cells by PPARδ ameliorates obesity-induced insulin resistance. *Cell Metab*. 2008;7:496-507. DOI PubMed PMC
111. Luo W, Xu Q, Wang Q, Wu H, Hua J. Effect of modulation of PPAR-γ activity on Kupffer cells M1/M2 polarization in the development of non-alcoholic fatty liver disease. *Sci Rep*. 2017;7:44612. DOI PubMed PMC
112. Fang J, Li L, Cao X, et al. Transmissible endoplasmic reticulum stress mediated by extracellular vesicles from adipocyte promoting the senescence of adipose-derived mesenchymal stem cells in hypertrophic obesity. *Oxid Med Cell Longev*. 2022;2022:7175027. DOI PubMed PMC
113. Park SW, Zhou Y, Lee J, et al. The regulatory subunits of PI3K, p85α and p85β, interact with XBP-1 and increase its nuclear translocation. *Nat Med*. 2010;16:429-37. DOI PubMed PMC
114. Puri P, Mirshahi F, Cheung O, et al. Activation and dysregulation of the unfolded protein response in nonalcoholic fatty liver disease. *Gastroenterology*. 2008;134:568-76. DOI PubMed
115. Fernandes-da-Silva A, Miranda CS, Santana-Oliveira DA, et al. Endoplasmic reticulum stress as the basis of obesity and metabolic diseases: focus on adipose tissue, liver, and pancreas. *Eur J Nutr*. 2021;60:2949-60. DOI PubMed
116. Auer H, Cabalo DG, Rodríguez-Cruces R, et al. From histology to macroscale function in the human amygdala. *Elife*. 2025;13:RP101950. DOI PubMed PMC
117. Gu Y, Zhang W, Hu Y, Chen Y, Shi J. Association between nonalcoholic fatty liver disease and depression: a systematic review and meta-analysis of observational studies. *J Affect Disord*. 2022;301:8-13. DOI PubMed
118. Shea S, Lionis C, Kite C, et al. Non-alcoholic fatty liver disease and coexisting depression, anxiety and/or stress in adults: a systematic review and meta-analysis. *Front Endocrinol*. 2024;15:1357664. DOI PubMed PMC
119. Qiao Y, Ding Y, Li G, Lu Y, Li S, Ke C. Role of depression in the development of cardiometabolic multimorbidity: findings from the UK Biobank study. *J Affect Disord*. 2022;319:260-6. DOI PubMed
120. Yang W, Li W, Wang S, et al. Association of cardiometabolic multimorbidity with risk of late-life depression: a nationwide twin study. *Eur Psychiatry*. 2024;67:e58. DOI PubMed PMC
121. Celikbilek A, Celikbilek M, Bozkurt G. Cognitive assessment of patients with nonalcoholic fatty liver disease. *Eur J Gastroenterol Hepatol*. 2018;30:944-50. DOI PubMed
122. Muzurović E, Peng CC, Belanger MJ, Sanoudou D, Mikhailidis DP, Mantzoros CS. Nonalcoholic fatty liver disease and cardiovascular disease: a review of shared cardiometabolic risk factors. *Hypertension*. 2022;79:1319-26. DOI PubMed
123. McCracken C, Raisi-Estabragh Z, Veldsman M, et al. Multi-organ imaging demonstrates the heart-brain-liver axis in UK Biobank participants. *Nat Commun*. 2022;13:7839. DOI PubMed PMC
124. Binesh A, Devaraj SN, Halagowder D. Atherogenic diet induced lipid accumulation induced NFκB level in heart, liver and brain of Wistar rat and diosgenin as an anti-inflammatory agent. *Life Sci*. 2018;196:28-37. DOI PubMed
125. Zheng J, Xu M, Yang Q, et al. Efficacy of metformin targets on cardiometabolic health in the general population and non-diabetic individuals: a Mendelian randomization study. *EBioMedicine*. 2023;96:104803. DOI PubMed PMC
126. Torres DM, Jones FJ, Shaw JC, Williams CD, Ward JA, Harrison SA. Rosiglitazone versus rosiglitazone and metformin versus rosiglitazone and losartan in the treatment of nonalcoholic steatohepatitis in humans: a 12-month randomized, prospective, open-label trial. *Hepatology*. 2011;54:1631-9. DOI PubMed
127. Cusi K, Orsak B, Bril F, et al. Long-term pioglitazone treatment for patients with nonalcoholic steatohepatitis and prediabetes or type 2 diabetes mellitus: a randomized trial. *Ann Intern Med*. 2016;165:305-15. DOI PubMed
128. Ito D, Shimizu S, Inoue K, et al. Comparison of ipragliflozin and pioglitazone effects on nonalcoholic fatty liver disease in patients with type 2 diabetes: a randomized, 24-week, open-label, active-controlled trial. *Diabetes Care*. 2017;40:1364-72. DOI PubMed

129. Cosentino F, Verma S, Ambery P, et al. Cardiometabolic risk management: insights from a European society of cardiology cardiovascular round table. *Eur Heart J.* 2023;44:4141-56. DOI PubMed

130. Wu S, Li Y, Zhang Y, et al. Sex and age differences in the association between metabolic dysfunction-associated fatty liver disease and heart failure: a prospective cohort study. *Circ Heart Fail.* 2024;17:e010841. DOI PubMed

131. Yeh ML, Yu ML. From nonalcoholic steatohepatitis, metabolic dysfunction-associated fatty liver disease, to steatotic liver disease: updates of nomenclature and impact on clinical trials. *Clin Mol Hepatol.* 2023;29:969-72. DOI PubMed PMC